NAVAL POSTGRADUATE SCHOOL

MONTEREY, CALIFORNIA

THESIS

PHASE ERRORS AND DOPPLER EFFECT IN DIGITAL COMMUNICATIONS

by

Chee Wai Ng

December 2007

Thesis Advisor: Tri Ha
Co-Advisor: David Jenn

Approved for public release; distribution is unlimited

THIS PAGE INTENTIONALLY LEFT BLANK

REPORT DOCUMENTATION PAGE			Form Approved OMB No. 0704-0188
Public reporting burden for this collection of information is estimated to average 1 hour per response, including the time for reviewing instruction, searching existing data sources, gathering and maintaining the data needed, and completing and reviewing the collection of information. Send comments regarding this burden estimate or any other aspect of this collection of information, including suggestions for reducing this burden, to Washington headquarters Services, Directorate for Information Operations and Reports, 1215 Jefferson Davis Highway, Suite 1204, Arlington, VA 22202-4302, and to the Office of Management and Budget, Paperwork Reduction Project (0704-0188) Washington DC 20503.			
1. AGENCY USE ONLY ***(Leave blank)***	**2. REPORT DATE** December 2007	**3. REPORT TYPE AND DATES COVERED** Master's Thesis	
4. TITLE AND SUBTITLE Phase Errors and Doppler Effect in Digital Communications			**5. FUNDING NUMBERS**
6. AUTHOR(S) Chee Wai Ng			
7. PERFORMING ORGANIZATION NAME(S) AND ADDRESS(ES) Naval Postgraduate School Monterey, CA 93943-5000			**8. PERFORMING ORGANIZATION REPORT NUMBER**
9. SPONSORING /MONITORING AGENCY NAME(S) AND ADDRESS(ES) N/A			**10. SPONSORING/MONITORING AGENCY REPORT NUMBER**
11. SUPPLEMENTARY NOTES The views expressed in this thesis are those of the author and do not reflect the official policy or position of the Department of Defense or the U.S. Government.			
12a. DISTRIBUTION / AVAILABILITY STATEMENT Approved for public release; distribution is unlimited			**12b. DISTRIBUTION CODE**

13. ABSTRACT (maximum 200 words)

The rollout of IEEE 802.16e for high speed mobile communications poses challenges to the design of equalizers for a time-varying multipath fading channel.

This thesis investigates the effects of Doppler shift induced phase error in a wireless environment. It presents the performance of QPSK and MQAM waveforms with Doppler in a Rayleigh channel condition. It investigates the performance of ideal coherent modulation and pilot symbol-aided modulation in a Rayleigh channel with Doppler phase errors. The degradation in performance of pilot symbol-aided demodulation as compared to ideal coherent demodulation is presented. The study concludes with results of simulations of QPSK and MQAM waveforms in a Rayleigh Channel with Doppler phase errors.

14. SUBJECT TERMS Doppler Shift, Phase Error, Effects on OFDM Signal, Rayleigh Fading, Pilot Symbol-Aided Demodulation			**15. NUMBER OF PAGES** 65
			16. PRICE CODE
17. SECURITY CLASSIFICATION OF REPORT Unclassified	**18. SECURITY CLASSIFICATION OF THIS PAGE** Unclassified	**19. SECURITY CLASSIFICATION OF ABSTRACT** Unclassified	**20. LIMITATION OF ABSTRACT** UU

Standard Form 298 (Rev. 8-98)
Prescribed by ANSI Std. Z39.18

THIS PAGE INTENTIONALLY LEFT BLANK

Approved for public release; distribution is unlimited

PHASE ERRORS AND DOPPLER EFFECT IN DIGITAL COMMUNICATIONS

Chee Wai Ng
Civilian, Singapore Defence Science & Technology Agency
BEng., Nanyang Technological University, 1998

Submitted in partial fulfillment of the
requirements for the degree of

MASTER OF SCIENCE IN ELECTRICAL ENGINEERING

from the

NAVAL POSTGRADUATE SCHOOL
December 2007

Author: Chee Wai, Ng

Approved by: Tri Ha
Thesis Advisor

David Jenn
Co-Advisor

Jeffrey Knorr
Chairman, Department of Electrical and Computer Engineering

THIS PAGE INTENTIONALLY LEFT BLANK

ABSTRACT

The rollout of IEEE 802.16e for high speed mobile communications poses challenges to the design of equalizers for a time-varying multipath fading channel.

This thesis investigates the effects of Doppler shift induced phase error in a wireless environment. It presents the performance of QPSK and MQAM waveforms with Doppler in a Rayleigh channel condition. It investigates the performance of ideal coherent modulation and pilot symbol-aided demodulation in a Rayleigh channel with Doppler phase errors. The degradation in performance of pilot symbol-aided demodulation as compared to ideal coherent demodulation is presented. The study concludes with results of simulations of the QPSK and MQAM waveforms in a Rayleigh Channel with Doppler phase errors.

THIS PAGE INTENTIONALLY LEFT BLANK

TABLE OF CONTENTS

LIST OF FIGURES

LIST OF TABLES

THIS PAGE INTENTIONALLY LEFT BLANK

EXECUTIVE SUMMARY

The increase in demand for wireless networks has grown exponentially in recent years. The demand for high bandwidth connectivity between networks is rising because the deployment period is short. While mobile services are getting more popular, it is prudent that the service providers keep up the Quality of Services (QoS) as well as the bandwidth demand.

In the wireless environment, fading and multipath are two phenomena present in wireless channels. Both affect the wireless signal propagation and result in distorted signals at the receivers. The effect limits the data throughput in the wireless environment. In a mobile network, the mobile station or subscriber is not stationary at a location; it moves from one point to another. This movement of one station creates an additional phenomenon known as Doppler shift.

The thesis studies the effect of Doppler phase error on digital communications. The analysis of its occurrence and impact on the various digital modulation schemes are presented. It addresses the commonly employed models of the M-ary Phase Shift Keying (MPSK) and M-ary Quadrature Amplitude Modulation (MQAM). It shows the mathematical expressions of the bit error probabilities of MPSK and MQAM. The objective is to present detailed analyses of the Doppler phase error in digital communications.

Important modules in the digital modulations and demodulations were presented with explanations of how the information bits transverse through these described modules. The introduction of Doppler shift in the transmission channel induced phase errors into the received signals. The effect of the phase error results in a rotation of the signal constellation. The analysis of the performances of the various MPSK and MQAM with phase error on an all white Gaussian noise (AWGN) channel and a Rayleigh fading channel are discussed. Doppler shift

induced phase errors degrade the performance of both MPSK and MQAM. It has greater impact as the order of modulation increases. Thus systems require higher Signal-to-Noise (SNR) to achieve equivalent throughputs.

The analysis of the relationship between Doppler spread and coherence time is presented. The definition of fast fading and slow fading based on Doppler spread and coherence time are discussed. The understanding of the effects of Doppler phase errors on the rotation of the constellations is paramount; it helps to visualize the change in the Euclidean distances in the constellations. It affects the performance of the decision points in the demodulation of the symbols. This thesis also provides an analysis and discussion on the Doppler effects in a Rayleigh fading channel. It includes the analysis on the performance of ideal coherent demodulation in a Rayleigh fading channel, followed by the analysis of an ideal coherent demodulation in a slow-flat Rayleigh fading channel and Doppler phase errors. The signal demodulation with pilot symbol-aided demodulation in a slow-flat Rayleigh channel and Doppler phase error is discussed. The performance of this technique was found to be degraded as compared to ideal coherent demodulation.

The analyses were verified with simulations. The simulator was developed in Matlab® and the various transmission scenarios were created through the definition of the channel and the receiver parameters. The results of the simulations confirm the theoretical analysis.

ACKNOWLEDGMENTS

First, I would like to offer my thanks to Professor Ha for his expertise and patience while helping me to complete this thesis

I would like thanks to my beloved wife, Siew Choo, and my boy, Wayne, who patiently endured my stress and absence during my research and study at NPS. I appreciate their love and concerns to keep my body healthy while working through the academic period.

Last but not least, I wish to thank to the Singapore Defence Science and Technology Agency (DSTA) for giving me this opportunity in experiencing a meaningful academic life at NPS.

THIS PAGE INTENTIONALLY LEFT BLANK

I. INTRODUCTION

A. BACKGROUND

The increase in demand of wireless networks has grown exponentially in recent years. The demand for high bandwidth connectivity between networks is rising because the deployment period is short. The IEEE 802.16a standard was created in 2003, to provide high broadband wireless internet access to metropolitan area networks (MANs). These wireless MANs (WMANs) provide point to multipoint access and optional mesh topology broadband wireless access.

Fading and multipath are two phenomena present in wireless channels. Both affect the wireless signals and result in distorted signals at the receivers. The effect limits the data throughput in the wireless environment. In a mobile network, the mobile station is not stationary at a location, it moves from one point to another. This movement of one station creates an additional phenomenon known as Doppler Shift. Doppler shift induces phase error in the received signals. The presence of Doppler phase error results in a rotation of the signal constellations. This affects the performance of the decision points in the demodulation of the symbols.

1. Doppler Shift

Doppler shift occurs due to a change in the observed frequency of a wave when the source and the receiver are in motion relative to each other. The frequency of the wave increases when the source and receiver approach each other and decreases when they move apart.

The Doppler effect has many uses in science and a variety of practical applications as well. Measurements of shifts of radio waves from orbiting satellites, for example, are used in maritime navigation, and the effect is also

employed in the radar surveillance of automobile speeds. In the medical field, the effect is used in such techniques as ultrasonography, or the study of motions in deep-lying body structures, and echocardiography, or the study of heart motions.

For mobile wireless applications, Doppler shift is created when there is relative velocity between transmitter and receiver. In this scenario, the propagation channel is time varying. The phase change in the received signal due to the difference in path length is

$$\Delta\phi = \frac{2\pi\Delta l}{\lambda} = \frac{2\pi v\Delta t}{\lambda}\cos\sigma \tag{1.1}$$

where $\Delta\phi$ is the phase variation during time Δt, σ is the angle between the direction of motion and direction of signal propagation and v is the velocity of motion. These are shown in Figure 1 for the case of a receiver in motion.

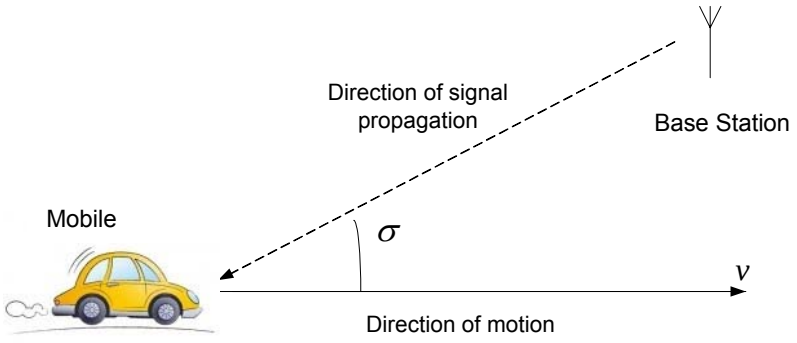

Figure 1. Doppler Shift in the Mobile Receiver

The Doppler shift is given by f_d, where v

$$f_d = \frac{1}{2\pi}.\frac{\Delta\phi}{\Delta t} = \frac{v}{\lambda}\cos\sigma = \frac{f_c v}{c}\cos\sigma \tag{1.2}$$

and c is the velocity of light in free space (3 x 10^8 m/s).

Equation (1.2) relates the Doppler shift to the mobile velocity and the spatial angle between the direction of motion of the mobile station and the direction of the wave. If the mobile receiver is moving towards the direction of

arrival of the wave, the Doppler shift is positive. However, if the mobile is moving away from the direction of arrival of the wave, the Doppler shift is negative.

B. OBJECTIVE

The objective of this study is to investigate Doppler induced phase errors for M-ary Phase Shift Keying (MPSK) and M-ary Quadrature Amplitude Modulation (MQAM) in all white Gaussian noise (AWGN) for Rayleigh fading channels. The performances of the modulations in the various channels were evaluated using pilot symbol-aided demodulation. In conclusion, we evaluated the results collected from a 802.16a simulator using Matlab® originally developed by Allen [1].

C. ORGANIZATION OF THESIS

This chapter is written to give the reader a brief overview of a Doppler shift and its implications to wireless communications. The rest of the thesis is organized as follows. Chapter II presents the Doppler effects on an AWGN channel. It presents the performance of the PSK, QPSK and MQAM modulations in the time-invariant channel. Chapter III presents Doppler effects in fading channels. This chapter evaluates the performance of the various modulation schemes in Rayleigh fading environments. Chapter IV presents the results of the performance evaluation of the various modulation techniques using a 802.16a simulator. It also discusses the degradation in performance of the modulation techniques when operating in the various fading channels. Chapter V presents the conclusions of the study and provides ideas for future work.

THIS PAGE INTENTIONALLY LEFT BLANK

II. PHASE ERRORS ON DIGITAL MODULATION

This chapter shows the effect of Doppler shift induced phase error on the received signals. It presents how the Doppler phase error effects the position of the symbols in the constellation and degrades the performance of the modulation schemes.

A. BACKGROUND

1. MPSK Signal

The basic MPSK signal is expressed as follows:

$$s_n(t) = A_p(t)\cos[2\pi f_c t + (2n-1)\tfrac{\pi}{M}] \tag{2.1}$$

where n = 1,2,3,…,M, M is the total number of symbols and f_c is the carrier frequency. Equation (2.1) can be expanded in terms of orthonormal basis functions

$$s_n(t) = A_p(t)\cos[(2n-1)\tfrac{\pi}{m}]\cos(2\pi f_c t) - A_p(t)\sin[(2n-1)\tfrac{\pi}{m}]\sin(2\pi f_c t) \tag{2.2}$$

Thus, $A_p(t)\cos\left[(2n-1)\tfrac{\pi}{m}\right]$ is the amplitude of the in-phase component (i.e., I-component) $\cos(2\pi f_c t)$, while $A_p(t)\sin\left[(2n-1)\tfrac{\pi}{m}\right]$ is the amplitude of the quadrature component (i.e., Q-component) $\sin(2\pi f_c t)$.

The typical block diagrams for a MPSK signal modulator and demodulator are shown in Figures 2 and 3, respectively.

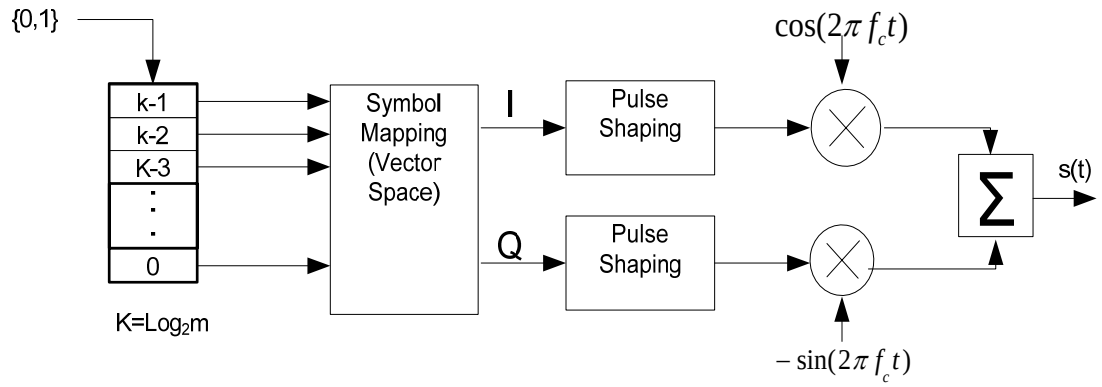

Figure 2. MPSK Modulator.

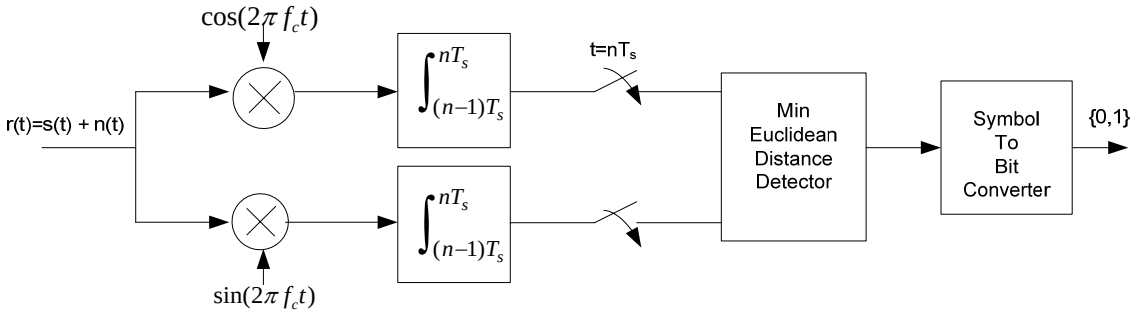

Figure 3. MPSK Demodulator.

In the modulator, the data bits are temporarily queued in a serial-to-parallel buffer. The size of the buffer corresponds to the number of bits k per symbol. This number relates to the M-levels of the modulation by $k = \log_2 M$. For example, for 16-level PSK, $k = \log_2 16 = 4$.

The data bits are passed to the symbol-to-mapping module at every symbol period, T_s, where $T_s = kT_b$ and T_b is the bit period. The symbol-to-mapping module translates the bits to the corresponding I-value and Q-value levels using the pre-assigned mapping. The pulse shaping band-limits the multi-level signals to a well-behaved signal with low inter-symbol interference (ISI).

These I and Q signals are then modulated with their respective orthogonal signals (cosine and sine carriers) to the required intermediate frequency (IF) and then to radio frequency (RF).

On the receiving end, the received signal is demodulated to base-band. Namely the I-signal and Q-signal are down converted with cosine and sine carriers. These base-band signals are filtered and time sampled at every symbol period T_S to recover the corresponding multi-level signals before they are mapped to the estimated points in the constellation using the minimum Euclidean distance (MED) detector module. The symbol-to-bit converter converts the symbols to the original data bits at a bit period of T_b.

2. MQAM Signal

The basic MQAM signal is expressed as follows:

$$s_n(t) = A_n P(t)\cos(2\pi f_c t + \theta_n) \tag{2.3}$$

where n = 1,2,3,…,M and M is the total number of symbols. $P(t)$ is the information bits. Equation (2.3) can be expanded via its orthonormal basis functions as:

$$s_n(t) = \alpha_n \cos(\theta_n) AP(t)\cos(2\pi f_c t) - \alpha_n \sin(\theta_n) AP(t)\sin(2\pi f_c t) \tag{2.4}$$

where $\alpha_n = A_n / A$ equals the signal amplitude (normalized to the smallest signal amplitude A). Thus, $\alpha_n \cos(\theta_n)$ is the amplitude of the I-component while $\alpha_n \sin(\theta_n)$ is the amplitude of the Q-component.

The typical block diagrams for the MPSK signal modulator and demodulator are similar to those for PSK. The main differences lie in the symbol mapping in the modulator and the symbol-to-bit converter in the demodulator.

3. Effects of Phase Error on a PSK Signal

Suppose the relative velocity between the transmitter and receiver station is 100 km/hr (60 mph), the operating frequency is 6 GHz and the incident angle is zero. The Doppler shift in the received signal, based on Equation (1.2) is

$$f_d = \frac{f_c v}{c}\cos\sigma = \frac{(6\times10^9)(100\times10^3)}{(3\times10^8)(60\times60)}\cos(0) = 556 \text{ Hz} \qquad (2.5)$$

Consider the channel data rate of 14.4 kbps with PSK. The bit period, T_b, is 69.4 μsec. The phase error, ϑ_{error} at the end of the first symbol bit is

$$\vartheta_{error} = 2\pi f_d T_s = 2\pi(556)(69.4\times10^{-6})$$

$$\vartheta_{error} = 0.040 \text{ rad} = 2.3°$$

This phase error will be accumulated through each symbol until the system re-synchronizes its frame.

The Doppler shift induced phase error contributes an extra parameter to the recovered signal. In the I-Q signals, a phase error will be multiplexed to the amplitudes of the multi-level signal.

In terms of signal constellations, the constellation of PSK will be rotated by the phase error as shown below in Figure 4. The Doppler effect on a PSK constellation is displayed in Figure 5.

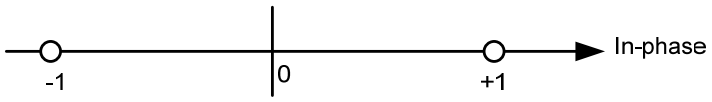

Figure 4. PSK Constellations.

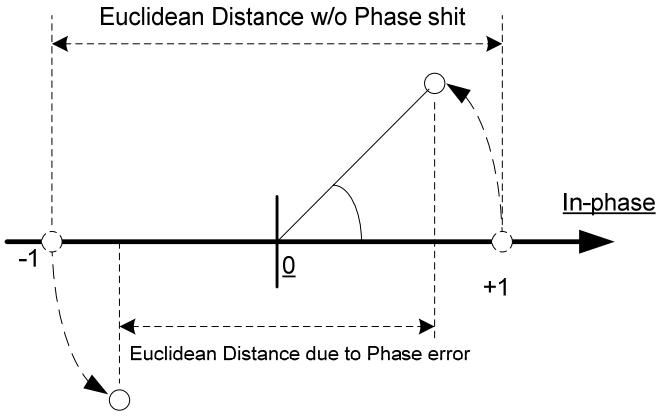

Figure 5. Doppler Effect on PSK Constellations.

Due to the Doppler effects on the transmitted signal, the received signals suffer phase shifts. This results in a distorted signal in the constellation which affects the symbol-to-bit mapping in the receiver and thus results in poorer bit error performance.

B. PERFORMANCE ANALYSIS OF PSK WITH PHASE ERRORS

With the phase error taken into consideration, the bit error probability for PSK with a phase error ϑ [2, 3] is

$$P_b(\vartheta) = Q\left(\sqrt{\frac{2E_b}{N_0}\cos^2\vartheta}\right) \tag{2.6}$$

Several curves are plotted in Figure 6.

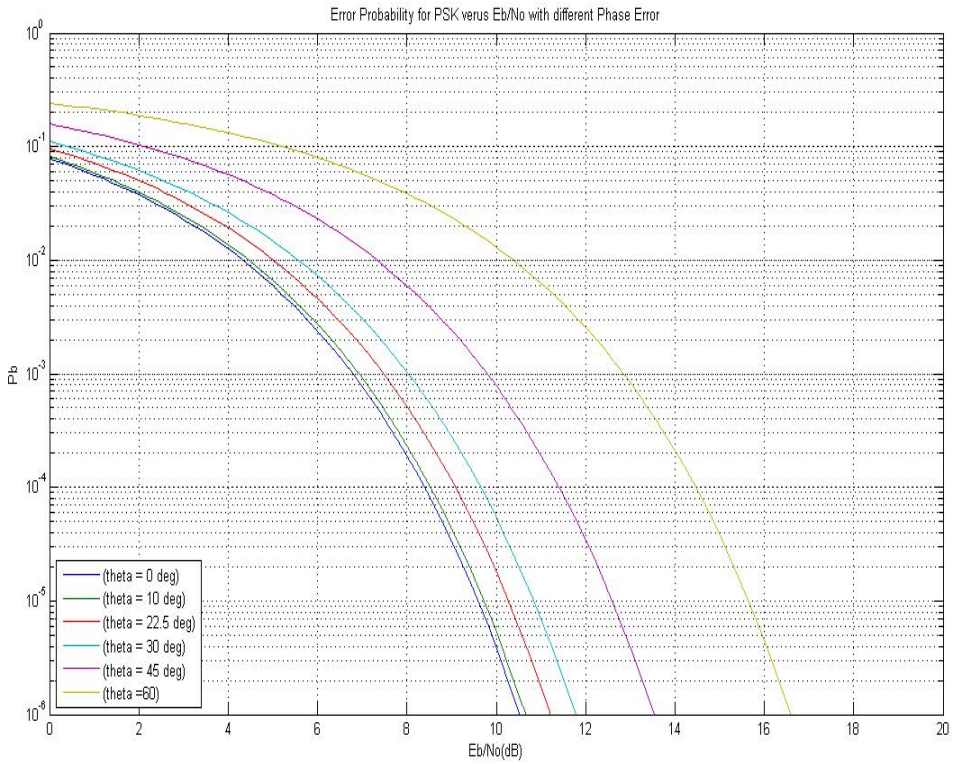

Figure 6. Bit Error Probability of PSK Signals with Various Phase Error.

From Figure 6, it is evident that the performance of PSK bit error rate deteriorates with an increase in phase error. The probability density function (PDF) of ϑ is assumed to be of the form [2],

$$f_{\vartheta}(\vartheta) = \begin{cases} \dfrac{\exp[x\cos\vartheta]}{2\pi I_0(x)}, & |\vartheta| \le \pi \\ 0, & \text{otherwise} \end{cases} \tag{2.7}$$

where $I_0(x)$ is a modified Bessel function of zeroth order, $x = 1/\sigma_{\vartheta}^2$ and σ_{ϑ}^2 is the variance of the phase error ϑ. Thus the bit error probability of the received signal is

$$P_b = \int P_b(\vartheta) f_{\vartheta}(\vartheta) d\vartheta \tag{2.8}$$

In Figure 7, the above bit error probability is plotted with the phase error standard deviations listed in Table 1.

σ_{ϑ} **(degrees)**	σ_{ϑ} **(radian)**
0	0
10	0.175
22.5	0.393
30	0.524
45	0.785
60	1.05

Table 1. Phase Error Standard Deviations

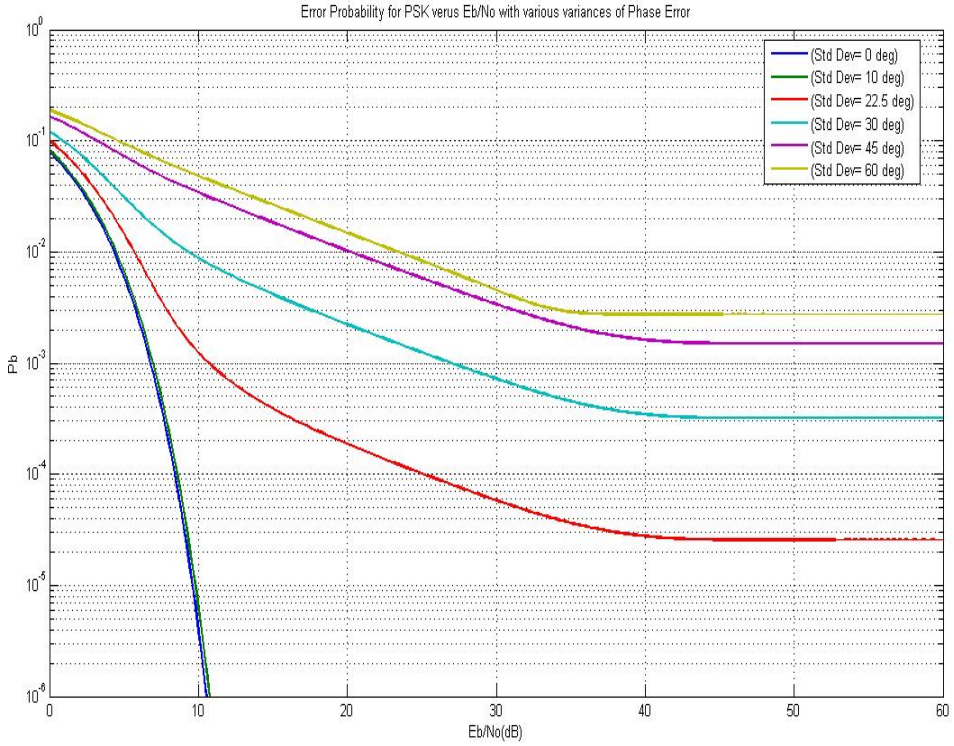

Figure 7. Bit Error Probability for Various Doppler Shift-Phase Errors on PSK Signals.

From Figure 7, it can be seem that the performance of the PSK modulation deteriorates as the σ_ϑ increases. It is noted that when σ_ϑ is greater than 22.5^o, the performance reaches steady state when E_b/N_o is greater than 40 dB.

C. PERFORMANCE ANALYSIS OF QPSK AND QAM SIGNALS WITH PHASE ERRORS

For QPSK and QAM signals, the constellations are a two-dimensional, as shown in Figure 8. The effect of Doppler shift results in rotation of the constellations. Figure 9 shows the phase error distortion of the Euclidean distances between the constellations. The constellation is rotated due to the phase error. The Euclidean distances in both the I- and Q-dimensions are affected and thus change the bit error performance in the receiver system.

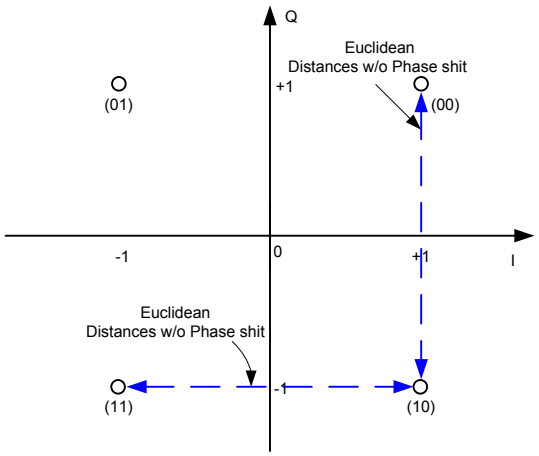

Figure 8. QPSK Constellation.

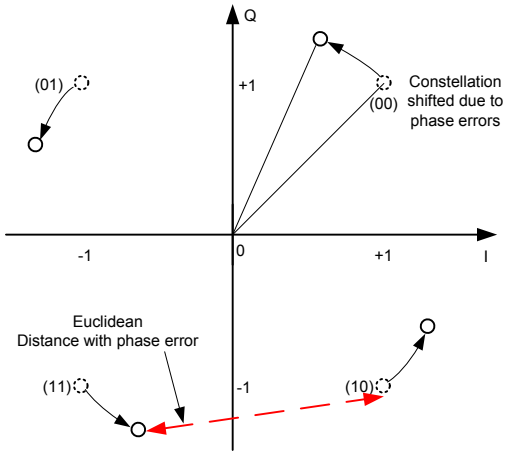

Figure 9. Phase Error Effect on a QPSK Constellation.

The bit error probability of QPSK and MQAM modulation [3] are as follows:

$$P_b(\vartheta) = \frac{N_n}{\log_2 M} Q\left(\frac{\boldsymbol{d}_{\min}(\vartheta)}{2\sigma}\right)$$

$$= \frac{N_n}{\log_2 M} Q\left(\sqrt{2\,SNR(\vartheta)}\right) \qquad (2.9)$$

where the signal-to-noise ratio (SNR) and the minimum Euclidean distance, $\boldsymbol{d}_{\min}(\vartheta)$, are

$$SNR(\vartheta) = \frac{1}{2}\left(\frac{\boldsymbol{d}_{\min}(\vartheta)}{2\sigma}\right)^2 \tag{2.10}$$

$$\boldsymbol{d}_{\min}(\vartheta) = \min_{i,j} \frac{\left\|\boldsymbol{T}_\vartheta \boldsymbol{s_i} - \boldsymbol{s}_j\right\|^2 - \left\|\boldsymbol{T}_\vartheta \boldsymbol{s_i} - \boldsymbol{s}_i\right\|^2}{\left\|\boldsymbol{s_i} - \boldsymbol{s}_j\right\|} \tag{2.11}$$

$$\boldsymbol{T}_\vartheta = \begin{pmatrix} \cos\vartheta & -\sin\vartheta \\ \sin\vartheta & \cos\vartheta \end{pmatrix} \tag{2.12}$$

where i and j are the reference symbol and its corresponding neighboring symbols in the constellation respectively. They take on values in Tables 2 to 4 depending on the modulation.

In addition, N_n is the average number of nearest neighboring symbols in the constellations and is defined as

$$N_n = 4 - \frac{4}{\sqrt{M}} \tag{2.13}$$

The coordinates of the QPSK signals are shown below in Table 2. The coordinates for 16QAM and 64QAM are in Table 3 and Table 4.

Signal s_i	I	Q
1	$+\sqrt{2}/2$	$+\sqrt{2}/2$
2	$-\sqrt{2}/2$	$+\sqrt{2}/2$
3	$-\sqrt{2}/2$	$-\sqrt{2}/2$
4	$+\sqrt{2}/2$	$-\sqrt{2}/2$

Signal Coordinates Normalized to $\sqrt{E_s}$

Table 2. Coordinates of QPSK Signal, s_i.

s_i	*I*	*Q*	s_i	*I*	*Q*	s_i	*I*	*Q*	s_i	*I*	*Q*
1	–3	–3	**4**	–1	–3	**9**	+1	–3	**13**	+3	–3
2	–3	–1	**6**	–1	–1	**10**	+1	–1	**14**	+3	–1
3	–3	+1	**7**	–1	+1	**11**	+1	+1	**15**	+3	+1
4	–3	+3	**8**	–1	+3	**12**	+1	+3	**16**	+3	+3

Signal Coordinates Normalized to $\sqrt{E}$

Table 3. Coordinates of 16QAM Signal, s_i.

s_i	*I*	*Q*	s_i	*I*	*Q*	s_i	*I*	*Q*	s_i	*I*	*Q*
1	–7	–7	**9**	–5	–7	**17**	–3	–7	**25**	–1	–7
2	–7	–5	**10**	–5	–5	**18**	–3	–5	**26**	–1	–5
3	–7	–3	**11**	–5	–3	**19**	–3	–3	**27**	–1	–3
4	–7	–1	**12**	–5	–1	**20**	–3	–1	**28**	–1	–1
5	–7	+1	**13**	–5	+1	**21**	–3	+1	**29**	–1	+1
6	–7	+3	**14**	–5	+3	**22**	–3	+3	**30**	–1	+3
7	–7	+5	**15**	–5	+5	**23**	–3	+5	**31**	–1	+5
8	–7	+7	**16**	–5	+7	**24**	–3	+7	**32**	–1	+7
s_i	*I*	*Q*	s_i	*I*	*Q*	s_i	*I*	*Q*	s_i	*I*	*Q*
33	+1	–7	**41**	+3	–7	**49**	+5	–7	**57**	+7	–7
34	+1	–5	**42**	+3	–5	**50**	+5	–5	**58**	+7	–5
35	+1	–3	**43**	+3	–3	**51**	+5	–3	**59**	+7	–3
36	+1	–1	**44**	+3	–1	**52**	+5	–1	**60**	+7	–1
37	+1	+1	**45**	+3	+1	**53**	+5	+1	**61**	+7	+1
38	+1	+3	**46**	+3	+3	**54**	+5	+3	**62**	+7	+3
39	+1	+5	**47**	+3	+5	**55**	+5	+5	**63**	+7	+5
40	+1	+7	**48**	+3	+7	**56**	+5	+7	**64**	+7	+7

Signal Coordinates Normalized to $\sqrt{E}$

Table 4. Coordinates of 64QAM Signal, s_i.

The relationship between the symbol energy, E_s, bit energy, E_b and the smallest symbol energy, E, is

$$E_s = E_b \log_2 M = \frac{1}{3}(M-1)E \tag{2.14}$$

Figures 10, 11 and 12 show the Doppler effects on the performance of the QPSK, 16QAM and 64QAM for the various phase errors shown in Table 1.

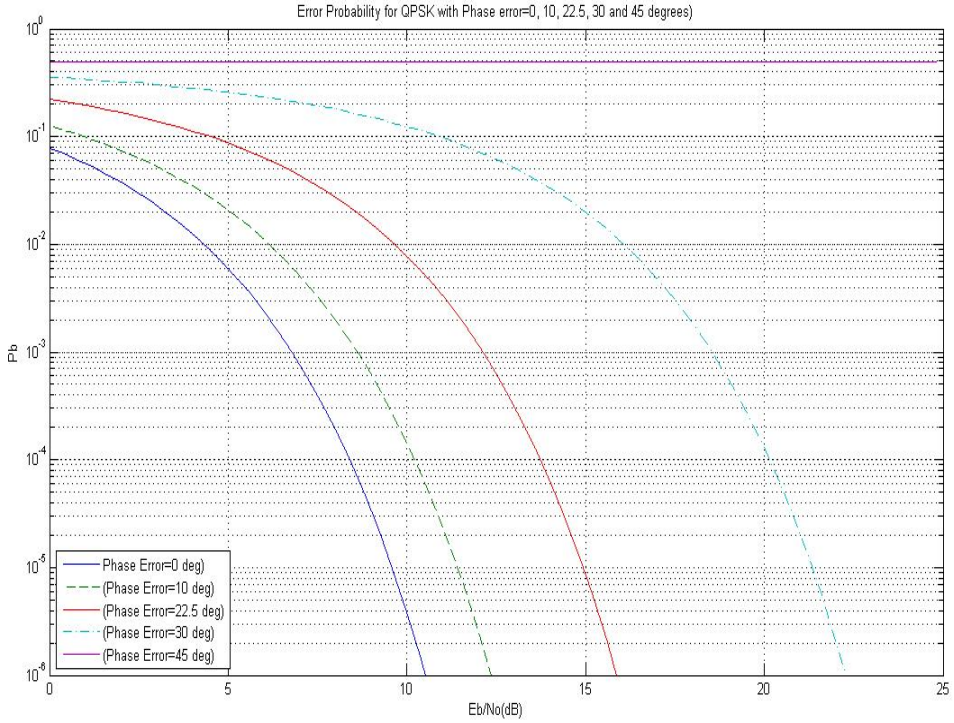

Figure 10. Bit Error Probability of QPSK Signals with Phase Errors.

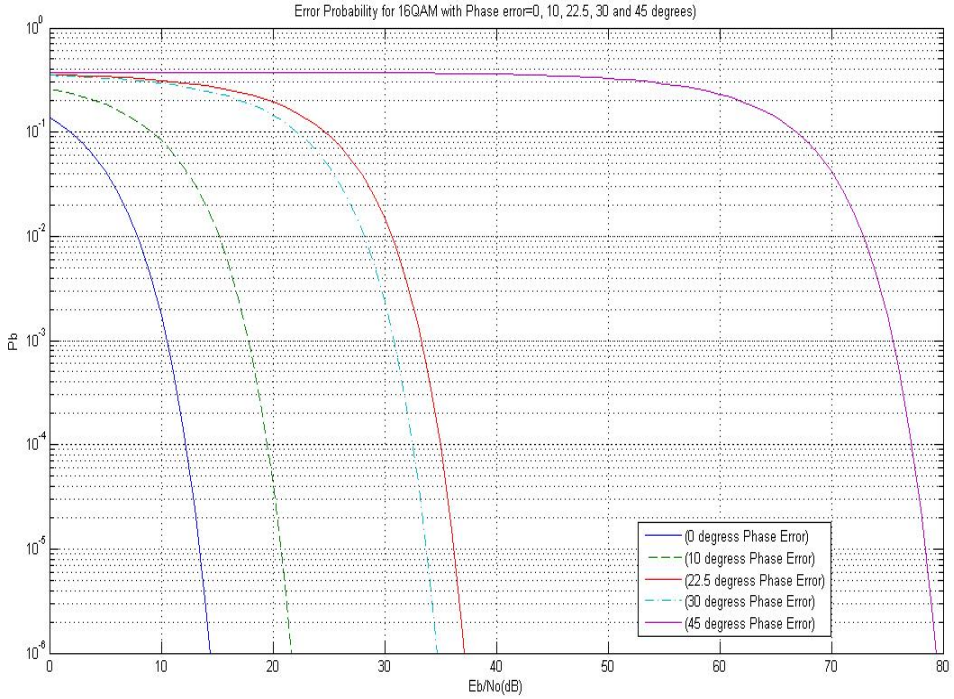

Figure 11. Bit Error Probability of 16QAM with Phase Errors.

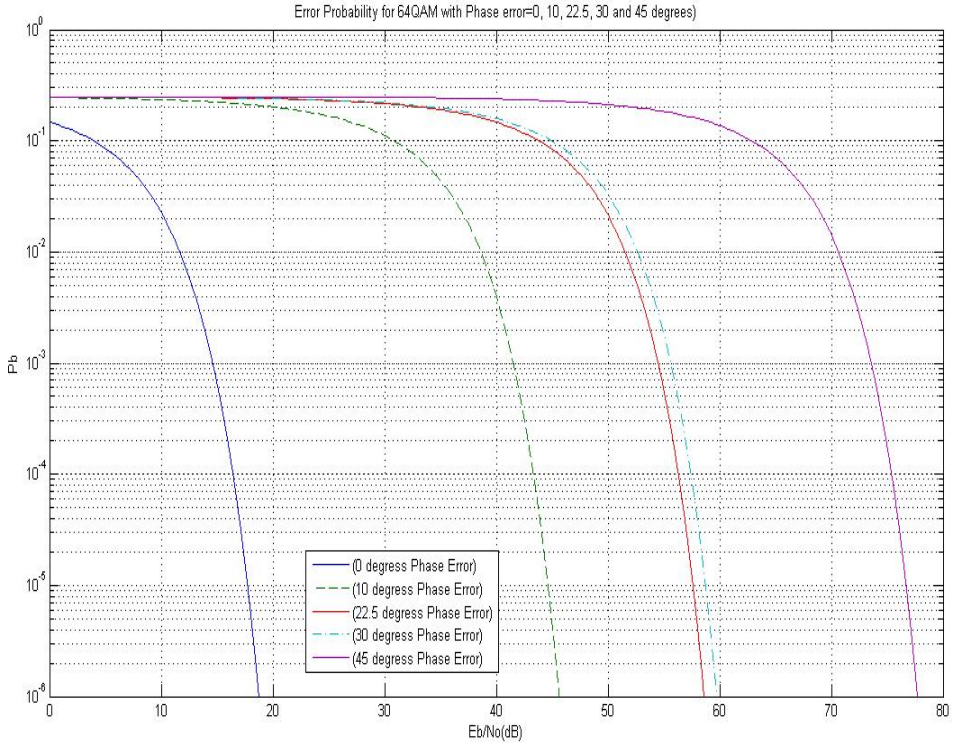

Figure 12. Bit Error Probability of 64QAM with Phase Errors.

The Doppler shift induced phase errors affect the performance of different modulation schemes. The performance of each modulation scheme deteriorates as the phase error increases. This is due to the phase error distorting the received signal and thus affects the position of signals in the constellations. As a result, the signal is incorrectly mapped by the receiver's MED detector.

Doppler shift has a greater impact on 64QAM as compared to 16QAM, and furthermore, the impact on QPSK is much less. As shown in the plots, for a 10^{-6} bit error rate (BER) performance, a 10^{o} phase error requires an additional 27 dB for 64QAM, an additional 7 dB for a 16QAM system, and only 2 dB more for QPSK.

In conclusion, this chapter shows the effect of Doppler shift induced phase errors on the received signals. It affects the positions of symbols in the constellation and thus degrades the performance of the modulation schemes. The impact is greater on the higher order modulations than the lower order modulations.

THIS PAGE INTENTIONALLY LEFT BLANK

III. DOPPLER EFFECTS IN FADING CHANNELS

This chapter evaluates the performance of various modulation schemes in a fading environment, mainly Rayleigh fading.

A. BACKGROUND

1. Doppler Spread and Coherence Time

The time varying nature of a channel in a small-scale fading region is defined by the channel Doppler spread and coherence time [4].

Doppler spread, f_D is a measure of the spectral broadening caused by the rate of change of the mobile channel. Doppler spread is defined as the maximum spectrum spread between all Doppler shifts of the propagation channel. In other words, it is the range of frequencies over which the received Doppler spectrum is essentially non-zero.

When a carrier of frequency, f_c, is transmitted, the Doppler spectrum has components in the range of $f_c - f_m$ to $f_c + f_m$, where f_m is the maximum Doppler shift given by $f_m = v/\lambda$. The amount of spectral spread depends on f_m. It can be expressed as:

$$f_D = \max_{i,j} | f_i - f_j | \tag{3.1}$$

where $f_i - f_j$ is the separation between two components in the Doppler spectrum. Thus

$$f_D = (f_c + f_m) - (f_c - f_m) = 2 f_m \tag{3.2}$$

If the bandwidth of a baseband signal is greater than f_D, the effects of the Doppler spread are negligible at the receiver [4]. This is known as a slow fading channel.

In the time domain, the coherence time is the dual of Doppler spread and is used to characterize the time varying property of the frequency spread (dispersion) of the channel in time. The Doppler spread and coherence time are inversely proportional to each other:

$$T_c \approx \frac{1}{f_m} \tag{3.3}$$

Coherence time is a statistical measure of the time duration over which the channel impulse response is essentially invariant, and quantifies the similarity of the channel response at different times. It is the period where two received signals have a strong potential for amplitude correlation. If the coherence time of the channel is smaller than the symbol time of the transmitted signal, the channel will change during the transmission of a symbol.

2. Fading Effects Due to Doppler Spread

There are two types of fading caused by Doppler spread: fast fading and slow fading. The main consideration is the relative difference between the symbol period T_s and the coherence time T_c which relates to the relative velocity between the transmitter and receiver.

In a fast fading channel, the channel impulse response changes rapidly within the transmitted symbol duration. Thus, the coherence time is smaller than the symbol time. The fluctuation distortion due to Doppler spread or frequency dispersion is significant and leads to signal distortion. Signal distortion increases as the Doppler spread increases in relation to the bandwidth of the transmitted signal.

A signal undergoes fast fading if

$$T_s > T_c \tag{3.4}$$

or

$$B_S < f_D \tag{3.5}$$

It is noted that fast fading occurs for very low data rates.

In a slow fading channel, the channel impulse response changes at a rate much slower than the transmitted baseband signal. In this case, the channel may be assumed to be static over one or several symbol periods. In the frequency domain, the Doppler spread of the channel is much less than the bandwidth of the baseband signal (B_s). Therefore, a signal undergoes slow fading if

$$T_s < T_c \tag{3.6}$$

or

$$B_S < f_D \tag{3.7}$$

Fast fading and slow fading can be summarized as in Table 5.

Small-Scale Fading (Based on Doppler spread)	
Fast Fading	***Slow Fading***
1. High Doppler Spread 2. Coherence Time < Symbol Period 3. Channel Variations Faster than Baseband Signal Variation	1. Low Doppler Spread 2. Coherence Time > Symbol Period 3. Channel Variations Slower than Baseband Signal Variation

Table 5. Summary of Fast Fading and Slow Fading.

3. Rayleigh Fading

In mobile channel modeling, statistical channel models are widely used to describe the time varying nature of the received envelope of a flat fading signal or the envelope of an individual multi-path component.

A Rayleigh distribution is widely used to describe the magnitude of the sum of two quadrature Gaussian noise signals. The Rayleigh distribution has a probability density function (pdf) given by

$$p(r) = \begin{cases} \dfrac{r}{\sigma^2}\exp\left(-\dfrac{r^2}{2\sigma^2}\right) & (0 \le r \le \infty) \\ 0 & (r < 0) \end{cases} \tag{3.8}$$

where $\mathbf{E}\left[r^2\right] = 2\sigma^2$ and $\mathbf{E}$ denotes the expected value.

In the next section, we shall analyze the performance with Doppler effects in Rayleigh fading channels.

B. PERFORMANCE ANALYSIS OF COHERENCE DEMODULATION IN RAYLEIGH FADING CHANNEL

1. PSK, QPSK and QAM with Ideal Coherent Demodulation in a Slow-Flat Rayleigh Fading Channel

For ideal coherent demodulation in a slow-flat Rayleigh fading channel, the bit error probability versus E_b / N_0 (dB) for PSK and QPSK [3] is:

$$P_b = \frac{1}{2}\left(1 - \sqrt{\frac{E_b / N_0}{1 + E_b / N_0}}\right) \tag{3.9}$$

and for MQAM:

$$P_b \approx \frac{2 - 2/\sqrt{M}}{\log_2 M}\left(1 - \sqrt{\frac{(3/2)[\log_2 M/(M-1)](E_b / N_0)}{1 + (3/2)[\log_2 M/(M-1)](E_b / N_0)}}\right) \tag{3.10}$$

These equations are plotted in Figure 13.

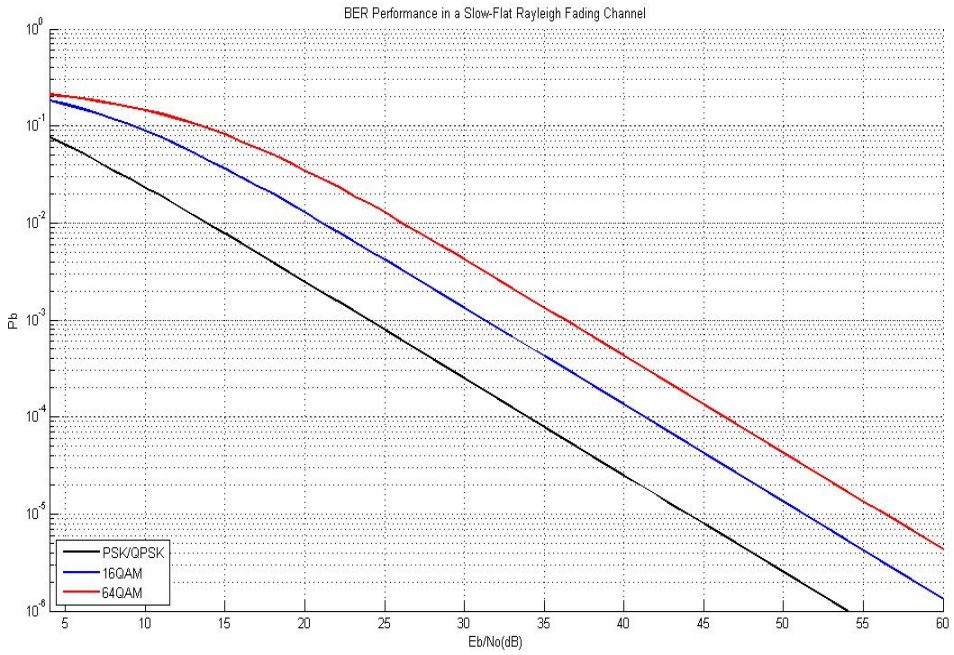

Figure 13. Bit Error Probabilities of Various Modulation Schemes with Ideal Coherent Demodulation in a Slow-Flat Rayleigh Fading Channel.

2. PSK, QPSK and QAM with Ideal Coherent Demodulation in a Slow-Flat Rayleigh Fading Channel and Doppler Phase Error

In this study, the impulse responses of the pilot and data channels are utilized where h_p is channel tap of the response of pilot channel while h_s is the channel tap for the data symbols channel response. It is assumed the magnitude of the channel taps for the pilot symbol, h_p, and the data symbol, h_s, are approximately equal, that is, $|h| = |h_p| \approx |h_s|$. This is the case when the amplitude fading rate is much smaller than the channel estimation rate, and when the pilot symbol is available from a parallel channel such as in IS-95 or IEEE 802.16a.

The bit error probability with a Doppler phase error, ε, and noise variance, σ^2, is given as [3]:

$$P_b(\varepsilon) = \mathbf{E}\left[P_b(|h|,\varepsilon)\right] \approx \mathbf{E}\left[\frac{N_n}{\log_2 M} Q\left(\frac{|h|\boldsymbol{d}_{\min}(\varepsilon)}{2\sigma}\right)\right]$$

$$\approx \mathbf{E}\left[\frac{N_n}{\log_2 M} Q\left(\sqrt{2|h|^2 SNR(\varepsilon)}\right)\right]$$

$$\approx \int \frac{N_n}{\log_2 M} Q\left(\sqrt{2|h|^2 SNR(\varepsilon)}\right) f_{|h|}(|h|)\, d|h| \qquad (3.11)$$

where $\mathbf{E}$ is the expected value, $\sigma^2 = N_0/2$, and $\boldsymbol{d}_{\min}(\varepsilon)$ and the signal-to-noise ratio (SNR) are defined as follows:

$$\boldsymbol{d}_{\min}(\varepsilon) = \min_{i,j} \boldsymbol{d}_{i,j}(\varepsilon) = \min_{i,j} \frac{\left[\left\|\boldsymbol{T}\boldsymbol{s}_i - \boldsymbol{s}_j\right\|^2 - \left\|\boldsymbol{T}\boldsymbol{s}_i - \boldsymbol{s}_i\right\|^2\right]}{\left\|\boldsymbol{s}_i - \boldsymbol{s}_j\right\|} \qquad (3.12)$$

$$SNR(\varepsilon) = \frac{1}{2}\left(\frac{\boldsymbol{d}_{\min}(\varepsilon)}{2\sigma}\right)^2 \qquad (3.13)$$

In addition, N_n is the average number of nearest neighboring symbols in the constellations and is defined as

$$N_n = 4 - \frac{4}{\sqrt{M}} \tag{3.14}$$

For all numerical results, it is considered that the channel tap $|h|$ is Rayleigh-distributed with density function

$$f_{|h|}(|h|) = 2|h|e^{-|h|^2} \tag{3.15}$$

In order to simplify our study, we normalize the channel tap such that $\mathbf{E}\left(|h|^2\right) = 1$.

a. Special Case of PSK

For PSK,

$$\boldsymbol{d}_{\min}(\varepsilon) = 2\sqrt{E_b}\cos\varepsilon \tag{3.16}$$

Figure 14 shows the performance of PSK versus E_b / N_0 (dB) in a Rayleigh fading channel for $\varepsilon = 0^0, 10^0, 22.5^0, 30^0$ and 45^0.

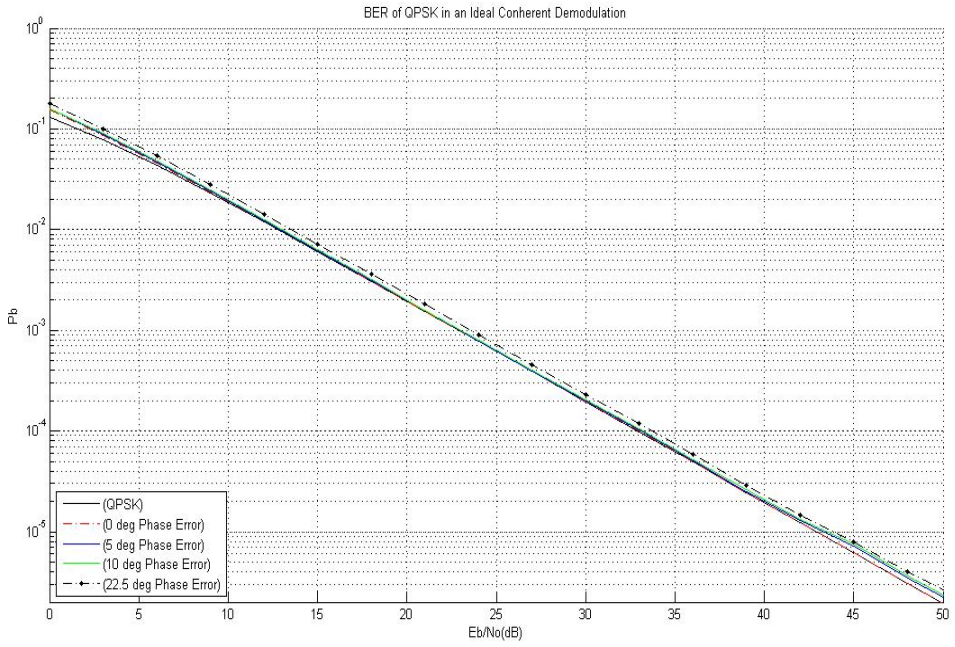

Figure 14. Bit Error Probability of PSK with Doppler Error in a Slow-Flat Rayleigh Fading Channel.

b. QPSK, 16QAM and 64QAM

The performances of the QPSK, 16QAM and 64QAM with ideal coherent demodulation in a Slow-Flat Rayleigh Fading Channel are shown in Figures 15, 16 and 17. The performance of each modulation scheme deteriorates as the Doppler phase error increases. It is shown that in each modulation scheme, higher SNR is required to achieve the required BER as the phase error value increases. It is also evident that the Doppler phase error distortion is greater in 64QAM as compared to 16QAM and likewise for 16QAM compared to QPSK. This is expected as the Euclidean distance is narrower in the constellation of higher order modulation schemes.

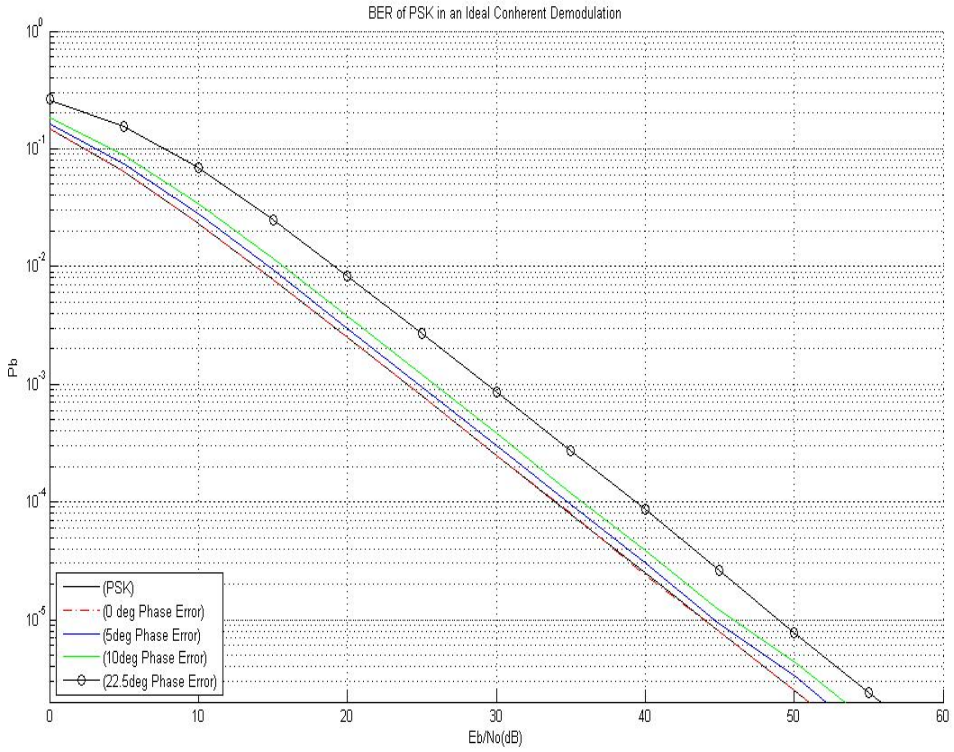

Figure 15. Bit Error Probability of QPSK in a Slow-Flat Rayleigh Fading Channel.

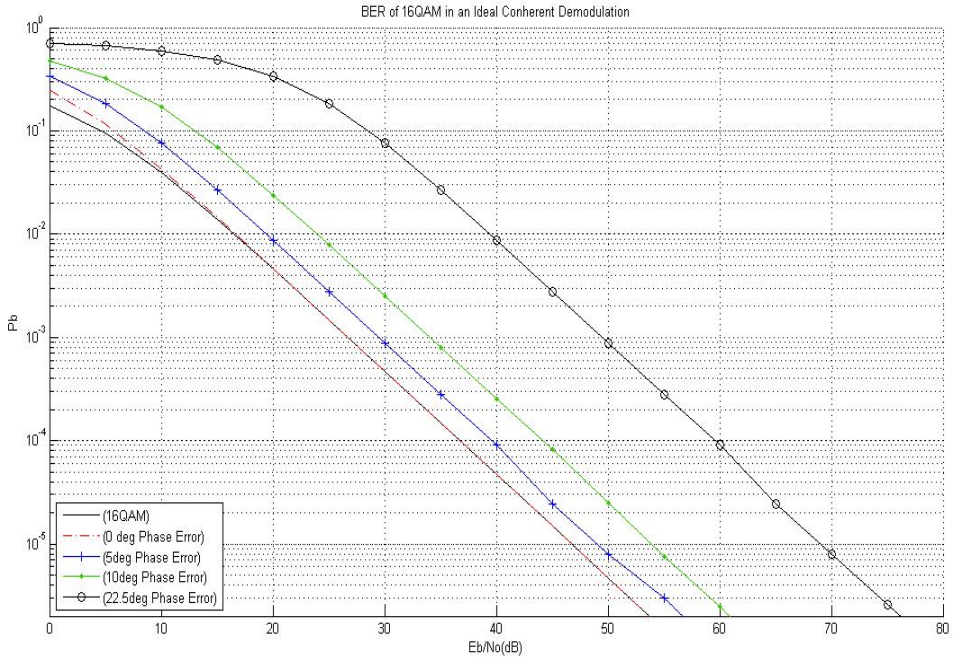

Figure 16. Bit Error Probability of 16QAM in a Slow-Flat Rayleigh Fading Channel.

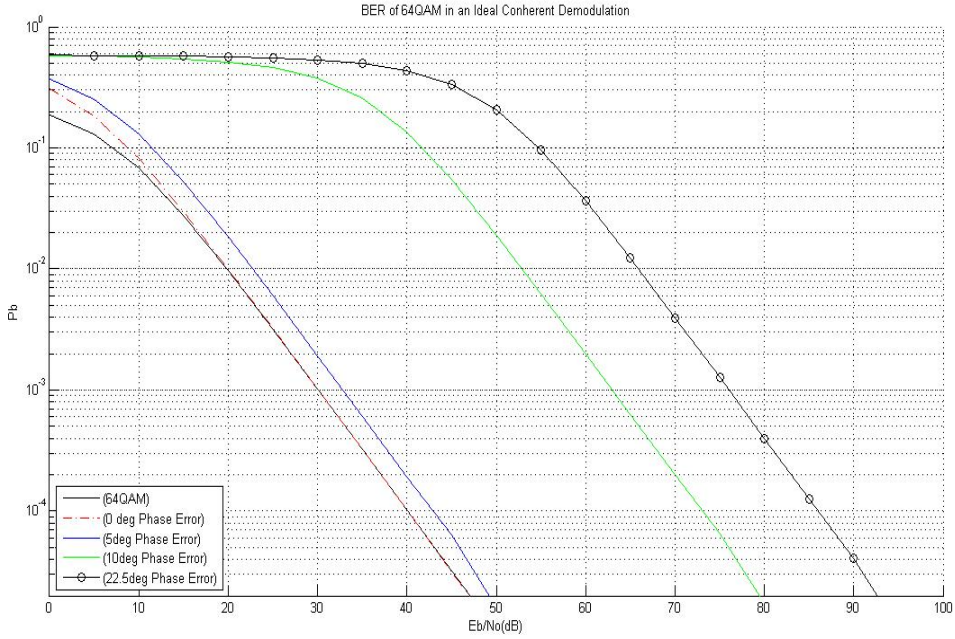

Figure 17. Bit Error Probability of 64QAM in a Slow-Flat Rayleigh Fading Channel.

Figures 18, 19 and 20 show a comparison of the performance of the various modulation schemes at 5^o, 10^o and 22.5^o Doppler phase error, respectively. It is evident that higher SNR is required to achieve the required BER when the Doppler phase error is greater. It is also observed that Doppler phase errors cause more distortion to the higher order modulation. Thus, the higher number modulation level schemes suffer more distortion with the same amount of Doppler phase error.

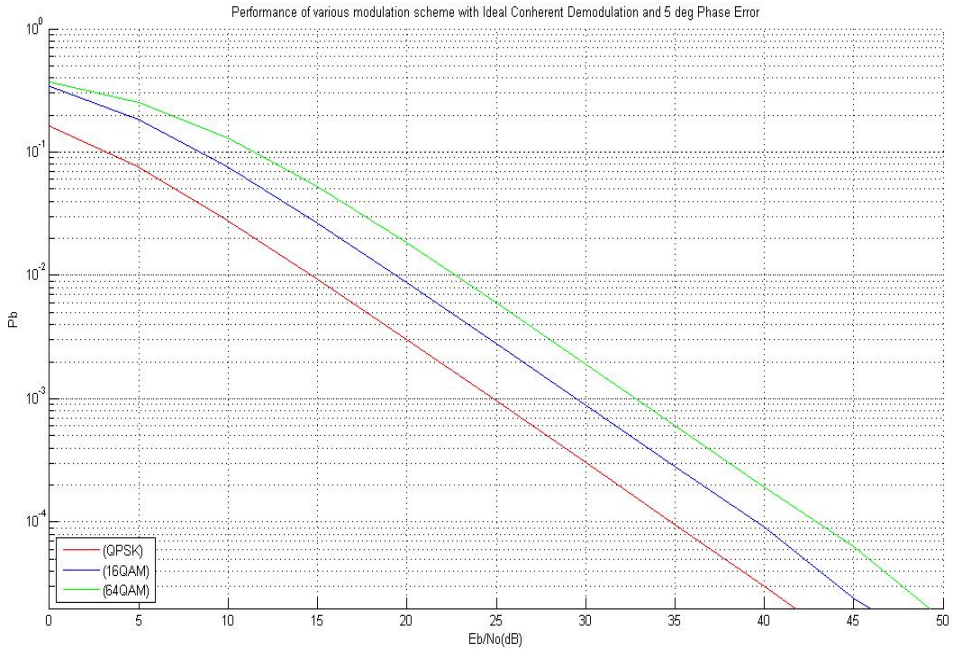

Figure 18. Bit Error Probability of Various Modulation Schemes at Phase Error of 5^o in a Slow-Flat Rayleigh Fading Channel.

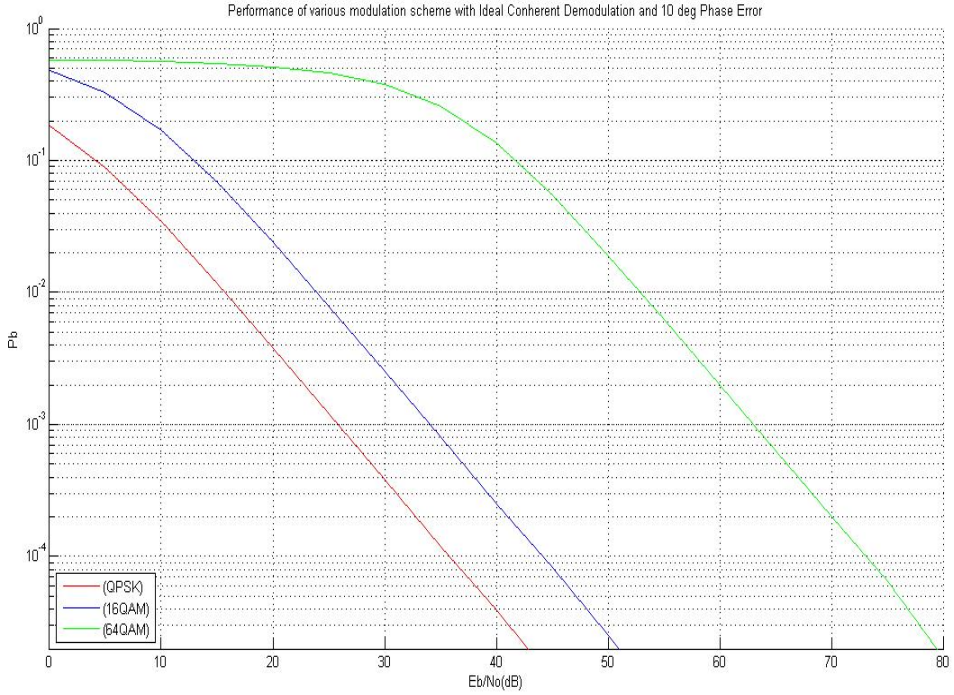

Figure 19. Bit Error Probability of Various Modulation Schemes at Phase Error of 10^{o} in a Slow-Flat Rayleigh Fading Channel.

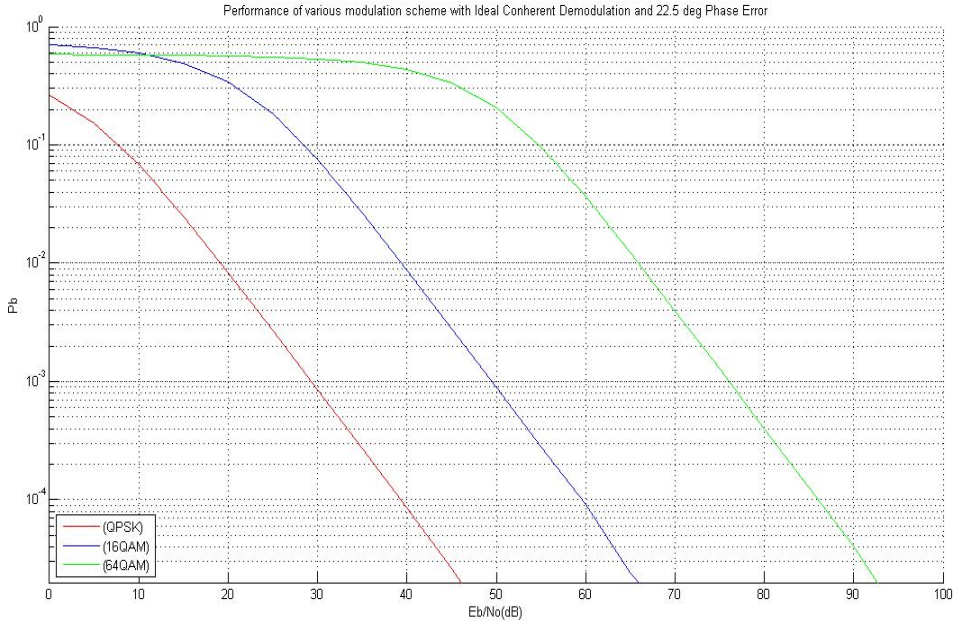

Figure 20. Bit Error Probability of Various Modulation Schemes at Phase Error of 22.5^{o} in a Slow-Flat Rayleigh Fading Channel.

Doppler shift has greater effect on 64QAM as compared to 16QAM, and similarly, a greater effect on 16QAM compared to QPSK. As shown in Figure 20, for a BER of 10^{-6} performance, a 64QAM system requires approximately an additional 28 dB as compared to 16QAM, while a 16QAM system requires an additional 20 dB as compared to QPSK system.

3. PSK, QPSK and QAM in a Slow–Flat Rayleigh Fading Channel with Pilot Symbol-Aided Demodulation and Doppler Phase Error

In this model, the magnitude of the channel taps for the pilot and data symbols are not equal, that is, $|h_p| \neq |h_s|$. This is the case when the amplitude fading rate is larger than the channel estimation rate and the pilot symbols are sent intermittently such as in Wideband Code Division Multiple Access (W-CDMA).

The bit error probability with a Doppler phase error ε and noise variance σ^2 [3] is:

$$P_b(\varepsilon) = \mathbf{E}\left[P_b\left(|h_p|,|h_s|,\varepsilon\right)\right] \approx \mathbf{E}\left[\frac{1}{\log_2 M}\sum_{i=1}^{M}\sum_{j=2}^{M}\Pr(H_i)Q\left(\frac{\boldsymbol{d}_{i,j}\left(|h_p|,|h_s|,\varepsilon\right)}{2\sigma}\right)\right]$$

$$\approx \int\int \frac{1}{M\log_2 M}\sum_{i=1}^{M}\sum_{j=2}^{M}Q\left(\frac{\boldsymbol{d}_{i,j}\left(|h_p|,|h_s|,\varepsilon\right)}{2\sigma}\right) f_{|h_p|}\left(|h_p|\right) f_{|h_s|}\left(|h_s|\right) d|h_p|\, d|h_s| \qquad (3.17)$$

where $\sigma^2 = N_0/2$, $P_r(H_i)$ and $\boldsymbol{d}_{i,j}\left(|h_p|,|h_s|,\varepsilon\right)$ are given by [2]:

$$P_r(H_i) = \frac{1}{M} \qquad (3.18)$$

$$\boldsymbol{d}_{i,j}\left(|h_p|,|h_s|,\varepsilon\right) = \frac{\left\|\,|h_s|\boldsymbol{T}\boldsymbol{s_i} - |h_p|\boldsymbol{s}_j\right\|^2 - \left\|\,|h_s|\boldsymbol{T}\boldsymbol{s_i} - |h_p|\boldsymbol{s}_i\right\|^2}{|h_p|\left\|\boldsymbol{s_i} - \boldsymbol{s}_j\right\|} \qquad (3.19)$$

Figures 21, 22 and 23 show the performance of the QPSK, 16QAM and 64QAM signals with pilot symbol-aided demodulation in a slow-flat Rayleigh fading channel with various Doppler phase errors. The performances degrade more than those in the ideal coherent demodulation at the same SNR.

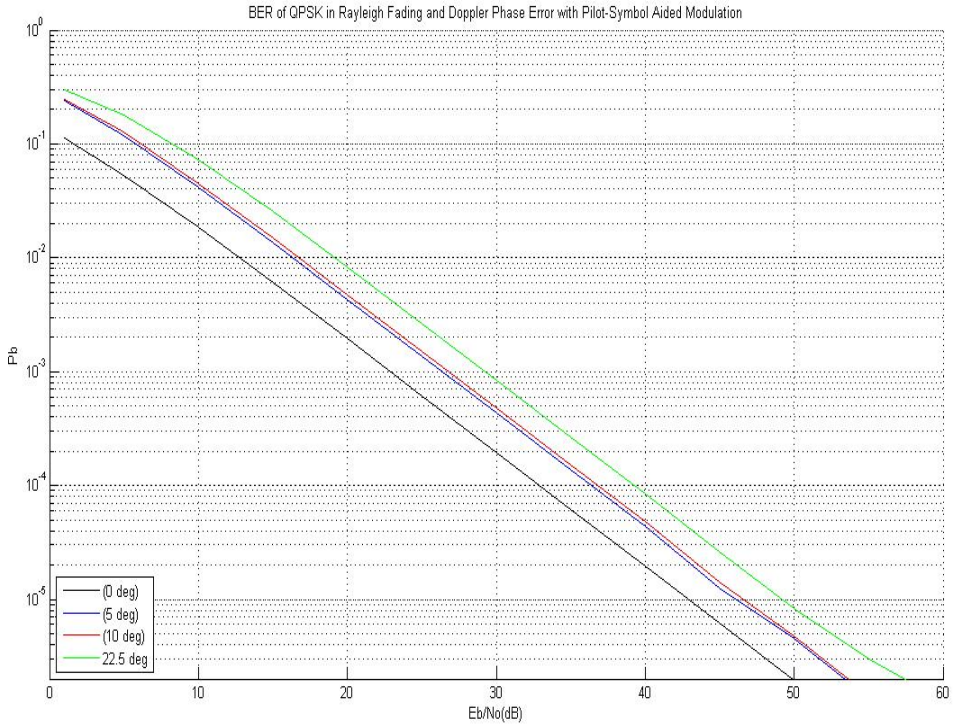

Figure 21. Bit Error Probability of QPSK in a Slow Flat Rayleigh Fading Channel with Pilot Symbol-Aided Demodulation and Doppler Phase Error.

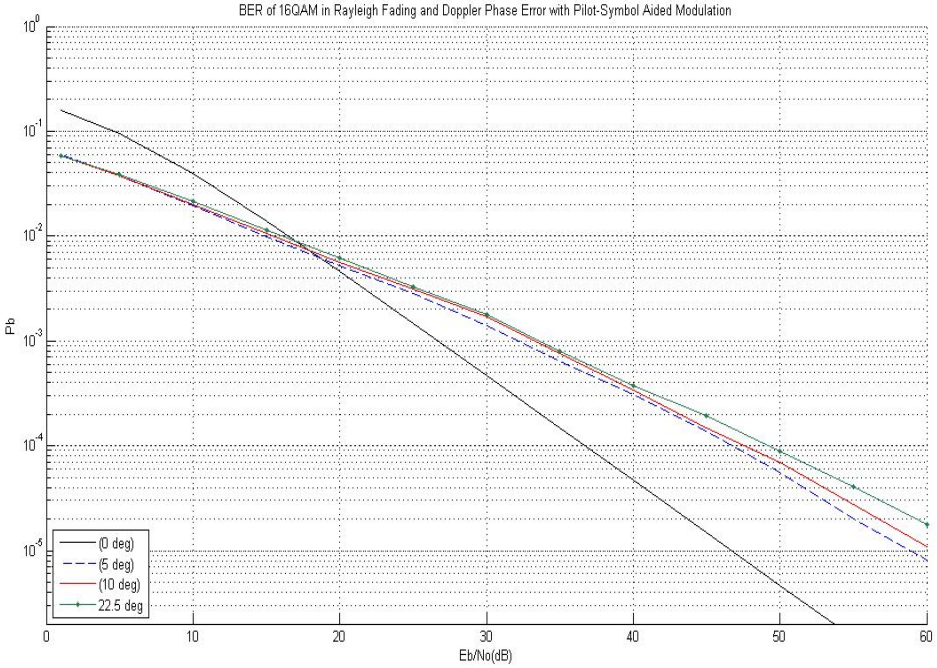

Figure 22. Bit Error Probability of 16QAM in a Slow-Flat Rayleigh Fading Channel with Pilot Symbol-Aided Demodulation and Doppler Phase Error.

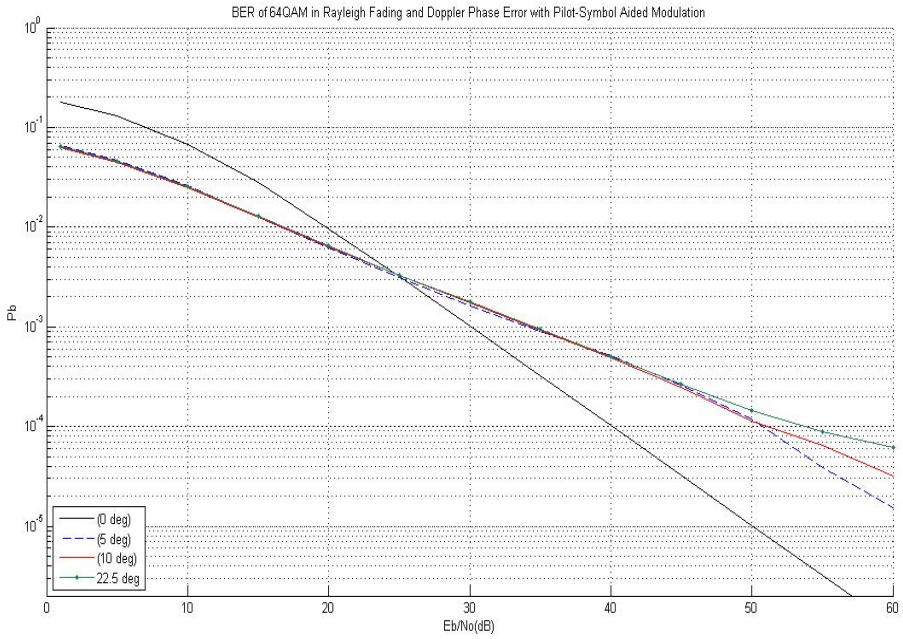

Figure 23. Bit Error Probability of 64QAM in a Slow-Flat Rayleigh Fading Channel with Pilot Symbol-Aided Demodulation and Doppler Phase Error.

Figures 24, 25 and 26 show the effects on the performance of the pilot symbol-aided demodulation for the various degrees of phase error. It is evident that the phase error affects the higher order modulation schemes more. This is because the constellations are very compact and a slight angle rotation will induce heavy distortions to the constellation thus resulting in a higher BER. The pilot symbols suffer similar Doppler phase errors as the data symbols, and thus lower the performance as compared to ideal coherent demodulation.

In conclusion, this chapter addressed the effect of a Doppler shift in a Rayleigh fading channel. It demonstrated the degradation of performance of the various modulation schemes. The performances of the ideal coherent demodulation and pilot symbol-aided demodulation in a Rayleigh channel with Doppler phase errors are presented. The performance of the pilot symbol-aided demodulation is poorer than the ideal coherent demodulation.

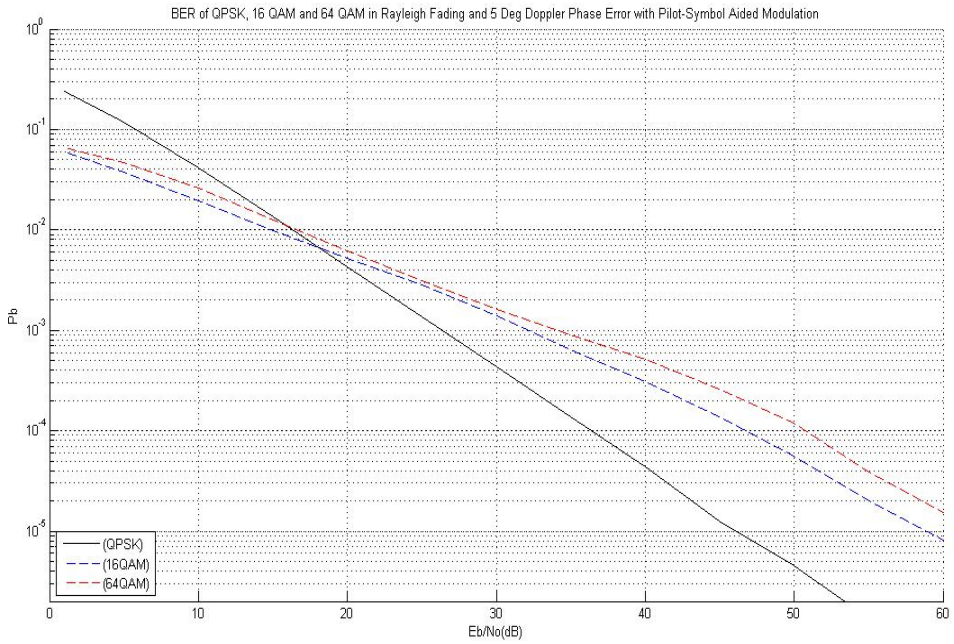

Figure 24. Bit Error Probability of Various Schemes at 5^{o} Doppler Phase Error in a Slow-Flat Rayleigh Fading Channel with Pilot Symbol-Aided Demodulation.

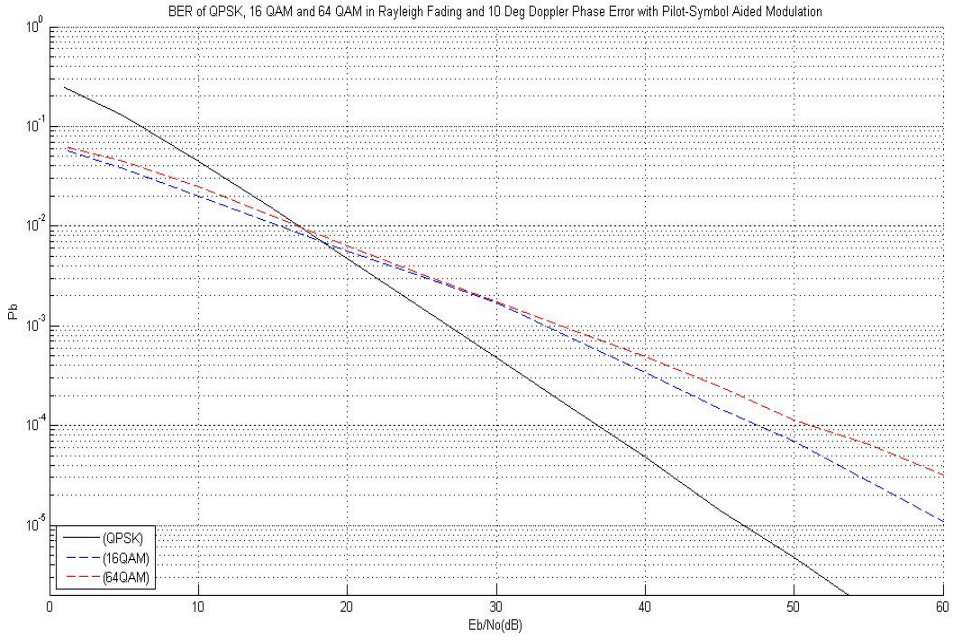

Figure 25. Bit Error Probability of Various Schemes at 10^{o} Doppler Phase Error in a Slow-Flat Rayleigh Fading Channel with Pilot Symbol-Aided Demodulation.

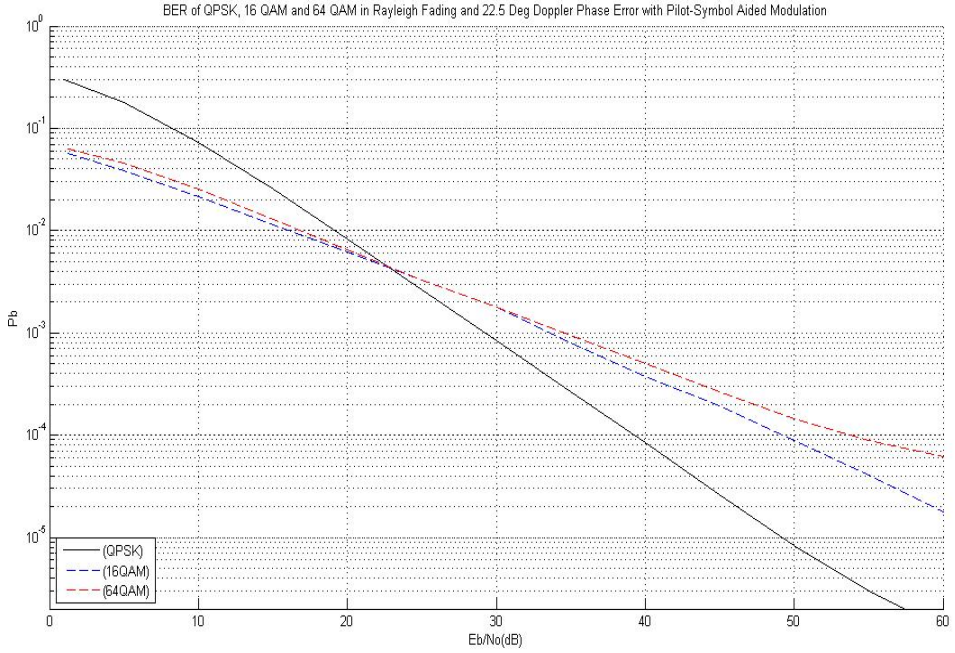

Figure 26. Bit Error Probability of Various Schemes at 22.5^{o} Doppler Phase Error in a Slow-Flat Rayleigh Fading Channel with Pilot Symbol-Aided Demodulation.

THIS PAGE INTENTIONALLY LEFT BLANK

IV. PERFORMANCE OF VARIOUS MODULATION TECHNIQUES USING SIMULATION

This chapter discusses the use of a simulator to evaluate the performance of various modulation schemes. The study employs a Monte Carlo simulation with a Matlab Graphical–User Interface (GUI). We modified the simulator used by Allen [1] from the GUI used in Segkos [5] to simulate IEEE 802.16a waveforms. In IEEE 802.16a, the modulation schemes are QPSK, 16QAM and 64QAM. These modulation schemes allow the system to offer variable bit rate in the range from 12 Mbps to 54 Mbps.

For the purpose of this work, the simulation duplicates the different environments and Doppler shift errors. The analysis focuses on the BER. Thus the simulation tracks the data bit prior to the modulation and after the demodulation and by passes coding and interleaving modules. This is for the purpose of comparing the results with those of previous chapters. All simulations are run on Rayleigh fading channels with no delay spread to simulate zero Inter-symbol Interference (ISI). The objective is to focus on the Doppler phase errors and their effects on various modulations schemes.

The simulation's cut off is based on meeting either one of the following two conditions:

1) Detection of at least 100 symbol errors, or

2) Transmission reached 10^8 data bits.

The following sections reproduce the scenarios created to verify the analysis as discussed in the Chapter III.

A. SIMULATION RESULTS OF PSK, QPSK AND QAM WITH IDEAL COHERENT DEMODULATION IN A SLOW-FLAT RAYLEIGH FADING CHANNEL

In this setup, the simulations were run with perfect synchronization and channel estimation. The channel environment is set to Rayleigh fading with zero delay spread. This will create a Rayleigh channel with zero ISI. The objective is to observe the performance of QPSK, 16QAM and 64QAM in a Rayleigh environment, prior to the introduction of Doppler shift errors.

The results were collected and compared to the analysis plots in Figure 13. Figure 27 shows simulation results of QPSK, 16QAM and 64QAM. The close agreement confirms the validity of the simulator.

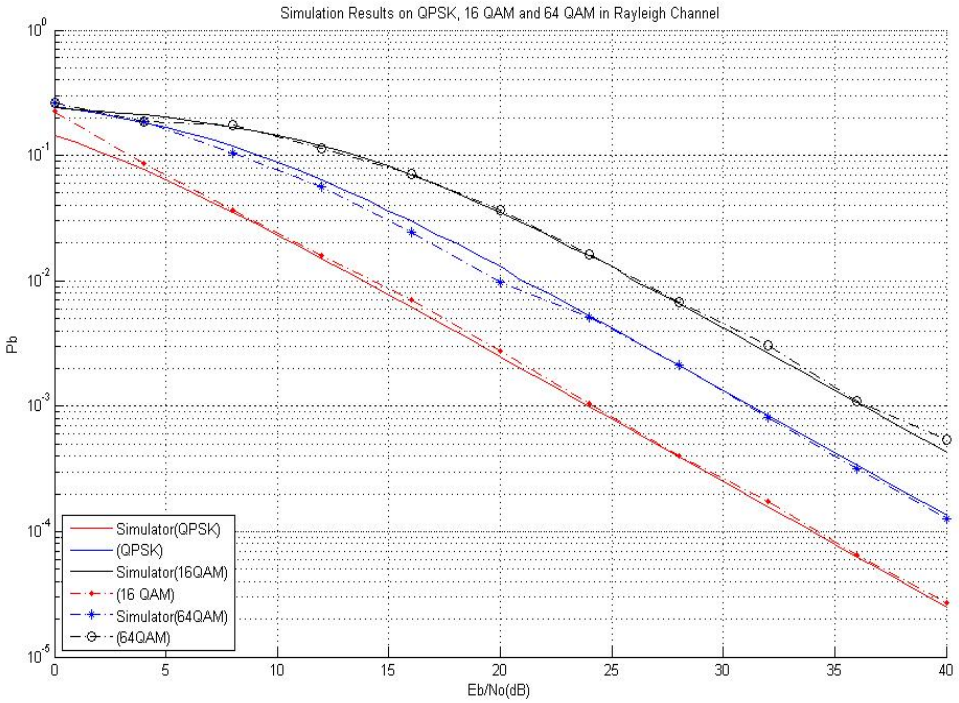

.

Figure 27. Simulation Results of QPSK, 16QAM and 64QAM in Rayleigh Fading Channel.

B. SIMULATION RESULTS OF QPSK AND QAM SUB-CARRIERS IN 802.16A WITH IDEAL COHERENT DEMODULATION IN A SLOW-FLAT RAYLEIGH FADING CHANNEL AND DOPPLER PHASE ERROR

In this setup, Doppler shifts were introduced to the channel. The simulation of the Doppler shift in a Rayleigh channel is performed by injecting an offset frequency onto the carrier frequency. This creates the relative frequency shift to the sub-carrier in 802.16a.

The simulation results for various modulation schemes were tabulated and plotted. Figures 28, 29 and 30 show the simulation results with reference to the results in the previous chapter. The results confirm the theoretical analysis discussed in Chapter III. The performance of the modulation schemes deteriorates as the amount of phase error increases from 5^{o} to 22.5^{o}. It also shows that the degradation increases from 16QAM to 64QAM.

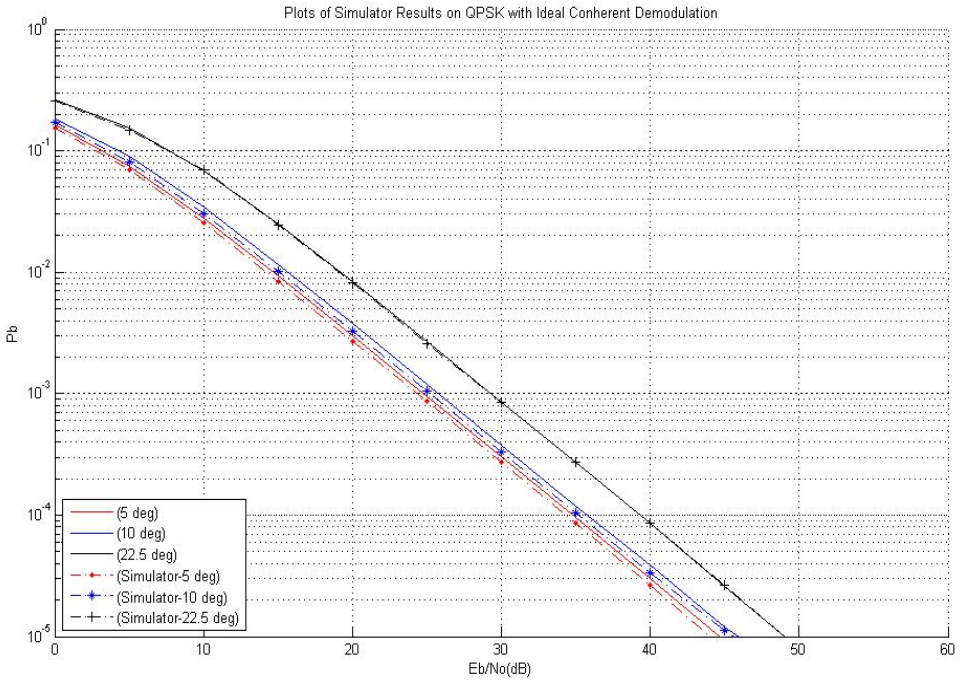

Figure 28. Simulation Results of QPSK in a Rayleigh Fading Channel with Doppler Phase Error.

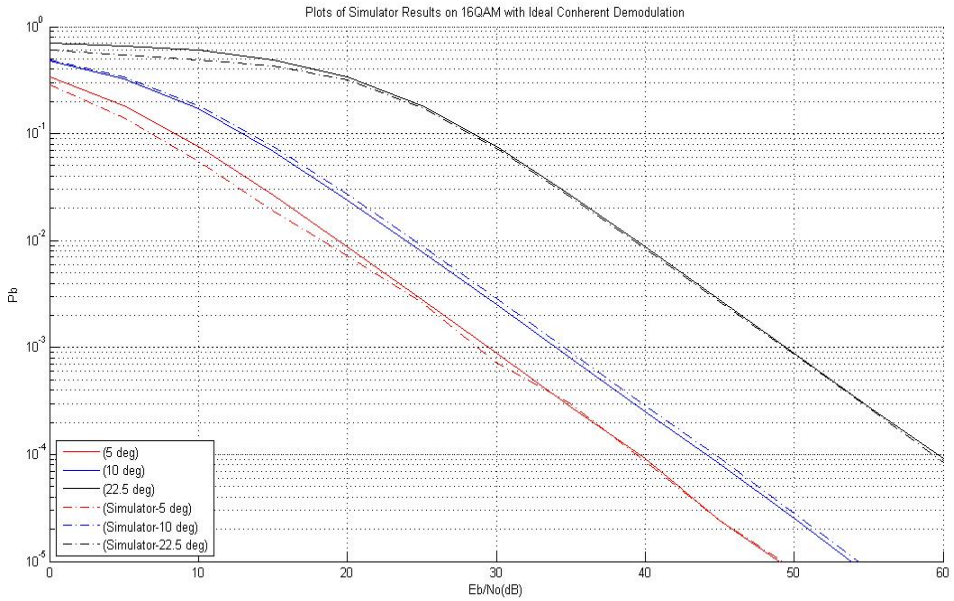

Figure 29. Simulation Results of 16QAM in a Rayleigh Fading Channel with Doppler Phase Error.

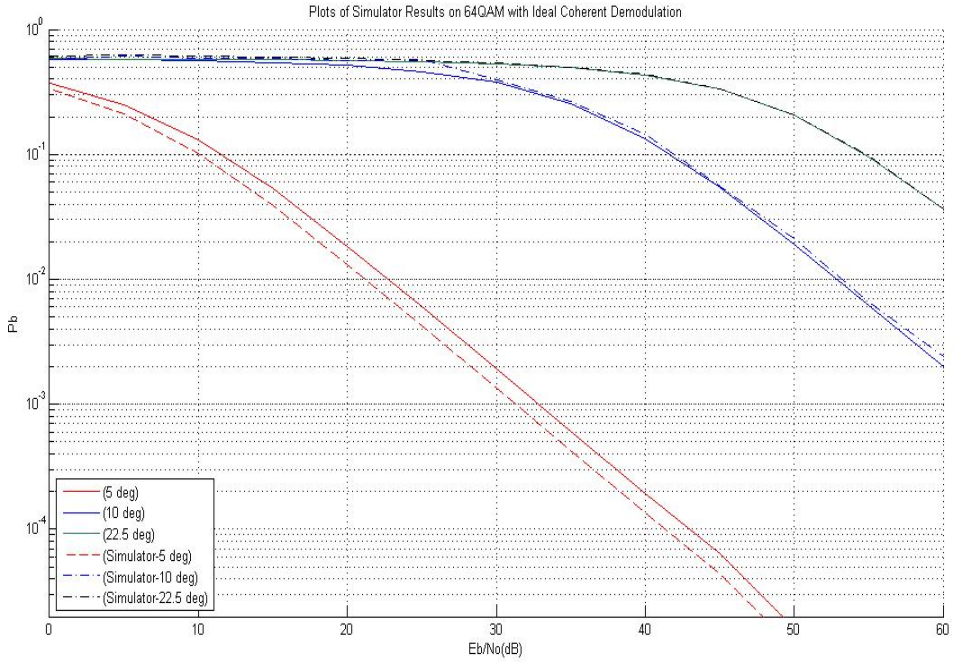

Figure 30. Simulation Results of 64QAM in a Rayleigh Fading Channel with Doppler Phase Error.

C. SIMULATION RESULTS OF QPSK AND QAM IN A SLOW–FLAT RAYLEIGH FADING CHANNEL WITH PILOT SYMBOL-AIDED DEMODULATION AND DOPPLER PHASE ERROR

In this setup, the synchronized module in the receiver is turned off and the receiver is set to use pilot symbol-aided demodulation to extract the phase of the received signals. The receiver extracts the synchronization with the pilot symbols in the transmitted pilot sub-carriers.

The simulation results for various modulation schemes were tabulated and plotted. Figures 31, 32 and 33 show the simulation results with reference to the analysis. It is evident by comparing these with Figures 28 to 30 that the performance of pilot symbol-aided demodulation is poorer than the ideal coherent demodulation.

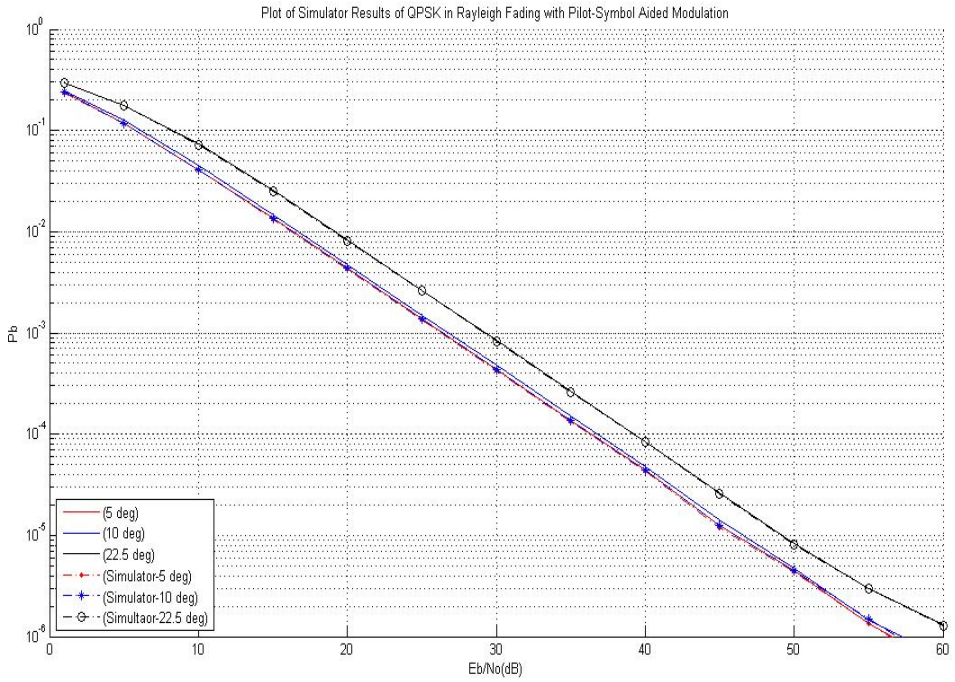

Figure 31. Simulation Results of QPSK with Pilot Symbol-Aided Demodulation in a Rayleigh Fading Channel with Doppler Phase Error.

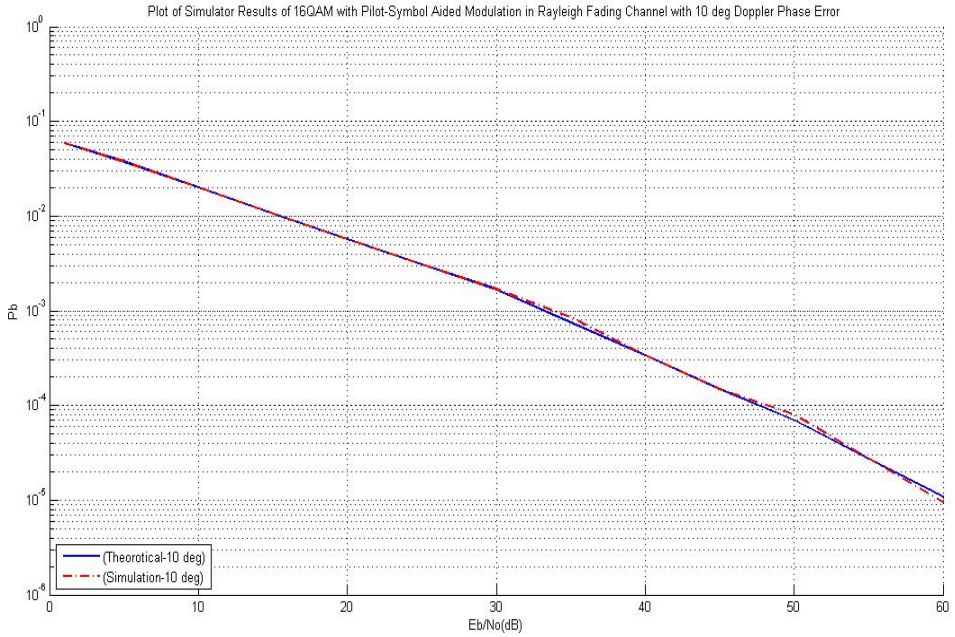

Figure 32. Simulation Results of 16QAM with Pilot Symbol-Aided Demodulation in Rayleigh Fading Channel with 10^{o} Doppler Phase Error.

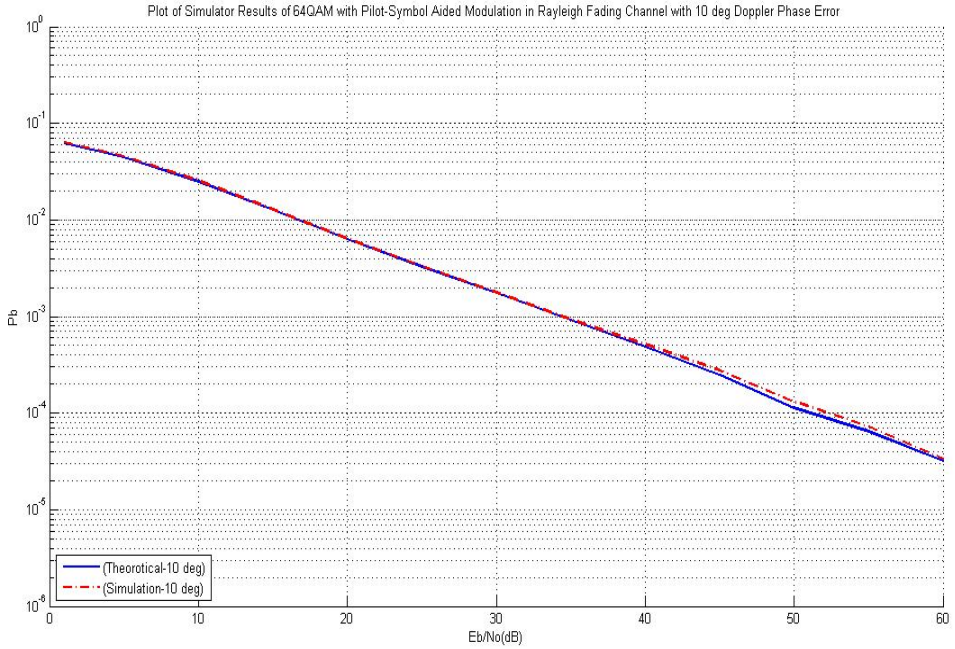

Figure 33. Simulation Results of 64QAM with Pilot Symbol-Aided Demodulation in a Rayleigh Fading Channel with 10^{o} Doppler Phase Error.

Doppler shifts induce phase errors that affect the performance of modulation schemes. The demodulation performance deteriorates as the amount of phase error increases. In addition, a higher order of modulation, such as 64QAM, suffers more degradation than a lower order modulation scheme, such as QPSK.

THIS PAGE INTENTIONALLY LEFT BLANK

V. CONCLUSION AND RECOMMENDATIONS FOR FUTURE WORK

A. CONCLUSION

A study on the effect of Doppler phase error on digital communications was presented in this thesis. The impact of the Doppler effect on the various digital modulation schemes was addressed.

Chapter II addressed the widely used MPSK and MQAM modulation schemes. It showed the mathematical expressions of bit error probability of MPSK and MQAM. Some of the important modules in the transmitter and receiver were presented, and how the data bits transverse through these modules was explained. The presence of a Doppler shift in the transmission channel induces phase errors into the received signal. The phase errors result in a rotation of the signal constellations. The analysis of the performance of MPSK and MQAM with phase errors in an AWGN channel was discussed. The Doppler shift induces phase errors and degrades the performance of both MPSK and MQAM. The Doppler shift has a greater impact on higher order modulations. This is due to the smaller Euclidean distances in the signal space and thus they are more prone to phase error distortion.

Chapter III discussed the relationship between Doppler spread and coherence time. The definitions of fast fading and slow fading based on Doppler spread and coherence time were presented. This chapter provided the analysis and discussion of the Doppler effect in a Rayleigh fading channel. It started with the analysis of the performance of ideal coherent demodulation in a Rayleigh fading channel. This was followed by the case of ideal coherent demodulation in a slow-flat Rayleigh fading channel with Doppler phase error. This chapter also included the performance of pilot symbol-aided demodulation in a slow-flat Rayleigh channel with Doppler phase error. The demodulation tracked the phase of the carrier through pilot symbols embedded in the pilot sub-carrier.

Chapter IV presented the simulation results of the Rayleigh environment as discussed in Chapters II and III. A 802.16a simulator was used as the tool for the simulation. The simulator was developed in Matlab® and the various transmission scenarios were created through the definition of the channel and the receiver parameters. The results of the simulations showed similar performances of various modulation schemes in the Rayleigh fading channel as described in the theoretical analysis.

This thesis showed that Doppler shift induces phase error that affects the performance of modulation schemes. As the amount of phase error increases, the system performance deteriorates. A higher order of modulation suffers more degradation than lower order modulation due to the compactness of its signal constellations. Ideal coherent demodulation offers better performance than pilot symbol-aided demodulation.

B. FUTURE WORK

There are many areas in which follow-on research is recommended. For instance, the study of Doppler shift phase errors in Nakagami and Rician channels.

In the area of cellular communications, one potential area of study is the effect of multiple Doppler phase errors from different base stations. This occurs when the subscriber is moving in the boundary areas between two base stations.

A diverse understanding of the effect of Doppler shift can greatly enhance the design of digital communications for airborne systems. Better systems can be deployed to improve mobile communications in both the military and commercial worlds.

LIST OF REFERENCES

[1] J. Allen, "*Performance Analysis of 802.16a*," M.S. thesis, Naval Postgraduate School, Monterey, CA, June 2005.

[2] Marvin K. Simon, *Digital Communications Techniques*, Prentice Hall, 1995.

[3] Tri T. Ha, *Digital Communications. Principles and Practice,* To be published.

[4] Theodore. S. Rappaport, *Wireless Communications,* 2nd edition, Prentice Hall, 2002.

[5] M. Segkos, "*Advance Techniques to improve the Performance of OFDM Wireless Lan*," M.S. thesis, Naval Postgraduate School, Monterey CA, June 2004.

[6] John G. Proakis, *Digital Communications*, 4th edition, Mc Graw Hill, 2001.

[7] Ramjee Prasad, *OFDM for Wireless Communications Systems*, Artech House, 2004.

THIS PAGE INTENTIONALLY LEFT BLANK

INITIAL DISTRIBUTION LIST

1. Defense Technical Information Center
   Ft. Belvoir, Virginia

2. Dudley Knox Library
   Naval Postgraduate School
   Monterey, California

3. Chairman, Department of Electrical and Computer Engineering, Code EC
   Naval Postgraduate School
   Monterey, California

4. Professor Tri Ha, Code EC/Ha
   Department of Electrical and Computer Engineering
   Naval Postgraduate School
   Monterey, California

5. Professor David Jenn, Code EC/Jn
   Department of Electrical and Computer Engineering
   Naval Postgraduate School
   Monterey, California

6. Chee Wai, Ng
   Defence Science and Technology Agency
   Singapore